2013-01-01

Inkjet Based Personalized Screening Platform For Cancer Therapy

Jorge Ivan Rodriguez
University of Texas at El Paso, jirodriguez6@miners.utep.edu

INKJET BASED PERSONALIZED SCREENING PLATFORM FOR CANCER THERAPY

JORGE IVAN RODRIGUEZ DEVORA

Program of Materials Science and Engineering

APPROVED:

_____
Thomas Boland, Ph.D., Chair

_____
Bill Tseng, Ph.D., Co-chair

_____
Felicia Manciu, Ph.D.

_____
Chuan Xiao, Ph.D.

_____
Jianying Zhang, Ph.D.

_____
Benjamin C. Flores, Ph.D.
Dean of the Graduate School

To my lovely wife and son, Daisy and Ian.

INKJET BASED PERSONALIZED SCREENING PLATFORM FOR CANCER THERAPY

by

JORGE IVAN RODRIGUEZ DEVORA, MS

DISSERTATION

Presented to the Faculty of the Graduate School of

The University of Texas at El Paso

in Partial Fulfillment

of the Requirements

for the Degree of

DOCTOR OF PHILOSOPHY

Program of Materials Science and Engineering

THE UNIVERSITY OF TEXAS AT EL PASO

May 2013

ACKNOWLEDGMENTS

First, I would like to express my deepest appreciation to Dr. Tao Xu for his training, guidance, friendship, and encouragement throughout this project. I would also like to express my sincere gratitude to my committee members: Dr. Thomas Boland, Dr. Bill Tseng, Dr. Jianying Zhang, Dr. Felicia Manciu, and Dr. Chuan (River) Xiao.

Additionally, I would like to specially thank the following individuals for assistance throughout the project: Daniel Reyna and Kabir M. Bhuyan. Moreover, the following individuals for their support and encouragement to gain new strengths for the completion of the project in many ways: Julio Rincon, Cesar Terrazas, Fabian Almeida, Maria Yañez, Ubaldo Robles, and Mireya Perez.

In addition, I would like to thank Dr. Thomas Boland, Dr. Lawrence Murr, Dr. Ahsan Choudhuri, Dr. Richard Schoephoerster, and Dr. Benjamin Flores for their support and continuous encouragement to let this kind of program continue with such progression within the university.

Finally, I would like to thank the following for providing funding for the completion of this adventure: the National Science Foundation (NSF), the University of Texas at El Paso, Department of Mechanical Engineering, the National Institute of Health (NIH), Chihuahua's Government special thanks to Mrs. Cesar Muñoz, and Mrs. Flor Marquez. Last but not least, I would like to thank Daisy for her unconditional love, support, and motivation to do an extra effort every day.

Inkjet Based Personalized Screening Platform for Cancer Therapy

ABSTRACT

by

JORGE IVÁN RODRÍGUEZ DÉVORA

The new paradigm of personalized medicine is beginning to affect clinical practice. In particular, many of the advances in genomics and proteomics have made personalized screening and therapeutic inventions possible. On chip, cellomics approaches to screening and intervention are becoming more commonplace. Cancer therapies may benefit from the rise in '-omics' technologies. In addition, the availability of rapid screening data is crucial to mitigate cancer propagation and increase the possibility of patient recovery. This study is an endeavor to develop a cellomic anticancer drug screening process based on inkjet printing. Previous research has demonstrated that inkjet based screening can reliably create isolated spots arrays at low volume (180 pl) and high throughput (213 spots/sec). Herein we study whether inkjet printing small volumes of anticancer drugs along with few cells has merit as a tool to fabricate cellomic chips. Inkjet printing has the potential to minimize drug use and maximize the use of cell biopsies.

Cells, from the hepatocellular carcinoma line HepG2 and the epithelial cell line PHEC, were printed with an inkjet device and thus arrayed on a 96-well plate for culture. The inkjet device was described before [1]. At mean exponential proliferation rate,

cyclophosphamide monohydrate (Cytoxan) and dichloroacetate sodium (DCA) at standard chemotherapeutic concentrations in the range of 1-50 mM were printed at continuously increasing densities in order to expose cultures to a drug concentration gradient. Anticancer drugs were studied under two solvents by means of dimethyl sulfoxide and PBS. The printed volumes were in the nanoliter range accounting for 625 ± 20% cells per spot. MTS assay was utilized to determine the amount of viable cells upon 24 hours of drug exposure followed by 48 hours for cell recovery. Half maximal and 90 percent inhibitory concentrations (IC50, IC90) were obtained from the dose-response curve. Along with the proposed cellomic chip, a screening platform using traditional micropipetting technique was built to compare results and validate inkjet based screening platform applicability.

Results obtained show that both cell lines were growth inhibited under both drug regimens. The IC50 values obtained by micropipetting and inkjet based screening varied less than 1mM suggesting that the proposed screening platform closely mimics the traditional screening outcome. However the IC90 values obtained vary in the range of 1 to 4.5 mM. The resulted IC50 indicates that 9.35 and 4.3 mM will be sufficient to inhibit growth of both cell lines under cytoxan and DCA treatment, respectively. In comparison to literature, IC50 results vary based on the cell lines used for the screening platform, but are generally in the range of 4-10 mM. Thus our results are consistent with those that used much larger volumes, validating our hypothesis that screening assays can be further miniaturized.

Inkjet technology shows promise to be used to determine dosages and treatment modalities using the patient's limited supply of biopsied cells. Expansion of the screening process to more drugs and usage of actual patients' biopsied cancer cells will result in valuable data to forecast efficiency of potential drug therapies.

TABLE OF CONTENTS

Page

LIST OF TABLES

Page

LIST OF FIGURES

Page

CHAPTER 1: INTRODUCTION

1.1 Personalized Medicine

Personalized medicine has gained attention in public health due to the continuous innovation in patient care. As a post-genomic era consequence, personalized medicine has emerged as a tailoring of medical treatment to the individual characteristics of each patient. This approach relies on scientific breakthroughs in the understanding of how a person's unique molecular and genetic profile makes them susceptible to certain diseases. This research is increasing our ability to predict which medical treatments will be safe and effective for each patient, and which ones will not [2]. Figure 1 shows a comparison of traditional against personalized medicine where treatment is improved by taking into account the particular onset conditions of the patient.

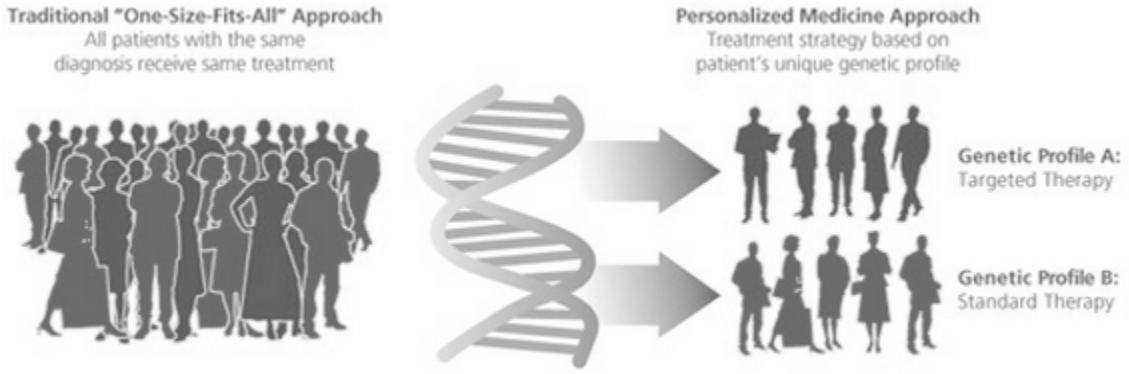

Figure 1.Personalized Medicine[3].

Personalized medicine can be classified based on the analysis level whether the focus be on cellomic (cytomic), proteomic, or genomic. While genomic and proteomic

approaches show more potential and scientific interest, due to the complexity of human genetic information this branch need further develop to transform itself into a clinical reality. One of the earliest and most common examples of personalized medicine at proteomic level came in Herceptin® (trastuzumab). In about 30% of patients with breast cancer over-express HER2, which is not responsive to standard therapy. Herceptin was approved for patients with HER2 positive tumors in 1998 and further research in 2005 showed that it reduced recurrence by 52% in combination with chemotherapy [4].

On the cellomic (cytomic) approach, cells constitute the elementary function unit. Diseases are caused by molecular changes in cells leading directly or indirectly to altered molecular cell phenotypes as a result of genotype and exposure influences during cell life. Cell phenotype changes may in a substantial number of instances be more closely linked to the actual disease process in individual patients and to its future development than either genomic status or environmental influences alone. Understanding the root causes of complex diseases such as cancer is essential for developing the most effective detection methods and for defining the most appropriate treatment (and ultimately preventive) strategies. The detection of some of these diseases has been greatly facilitated by the identification of diagnostic biomarkers, but until very recently, this approach focused largely on single molecules. In addition, a number of cancer therapies are targeted toward a specific molecule or signaling pathway, to inhibit tumor growth. These approaches reflect the traditional scientific approach of reducing cellular processes to their individual components and/or signal transduction pathways. However, the behaviors of most biological systems, including

those affected in cancer, cannot be attributed to a single molecule or pathway, rather they emerge as a result of interactions at multiple levels, and among many cellular components [5].

1.1.1 Personalized Medicine in Cancer Therapy

Cancer is the most devastating disease and leading cause of death throughout the world. Recent research has demonstrated that cancer has the greatest economic impact from premature death and disability of all causes of death worldwide [6]. The economic toll from cancer is nearly 20 percent higher than heart disease, the second leading cause of economic loss ($895 billion and $753 billion respectively). There is an increasing need for search of new compounds with selective cytotoxic effect on tumors whereas current anticancer drugs are often unsatisfactory due to the secondary toxic effect on healthy tissues. The lack of cancer-selective drugs and side effects tends to cause that cancer treatment results in an iterative process. Anticancer drug treatment prescribed by an oncologist depends on complex factors, such as type of cancer, aggressiveness, patient's weight, age, and physical condition, and often times based on socio-economic factors. Traditional medicine is focus on treatments based on the "one size fits all" model often neglecting individual on-set conditions that in some cases could even aggravate the disease treatment [1]. On the other hand, personalized medicine promises to refine diagnosis, guide optimum treatment, and avoid unnecessary side effects. While current anticancer drugs are developed based on *in vitro* studies made with commercially available cell lines, personalized medicine will require to study patient's own cells. In particular, there is need to develop miniaturized platforms to

analyze whether biopsied cancer cells are responsive to *in vitro* anticancer drugs to determine the appropriate dosage and drug formulations for treatment.

1.2 Drug Discovery Screening Process

The availability of high-speed, miniaturized, low-cost, and high throughput screening processes are very important issue in many fields such as drug discovery, biosensing, stem cell research, genomics, environmental monitoring, forensic investigation, and military defense [7, 8]. In drug discovery, surveys have been conducted in USA indicating that drug discovery and development costs have been rising. Although there are no fixed cost estimates, the most recent estimates stands at US$ 802 million [9] spread over 12 years or US$ 880 million distributed over 15 years [10] per single drug. A suggested probable reason for the rising in costs is that the new compounds are hard to synthesized, which limits the amount of assays that can be screen. Miniaturization of the screening process is required to optimize this process.

1.3 The Importance of Screening Process in Personalized Medicine

The pursuit of personalized medicine was one of the driving forces behind the 13-year, $3 billion Human Genome Project. Researchers hoped that once the genetic blueprint was revealed, they could create DNA tests to gauge individuals' risk for conditions like diabetes and cancer, allowing for targeted screening or preemptive intervention. Genetic information would help doctors select the right drugs to treat disease in a given patient. Such advances would dramatically improve medicine and

simultaneously lower costs by eliminating pointless treatments and reducing adverse drug reactions.

Personalized medicine is a young but rapidly advancing field of healthcare that is informed by each person's unique clinical, genetic, genomic, molecular, and environmental information. Because these factors are different for every person, the nature of diseases—including their onset, their course, and how they might respond to drugs or other interventions—is as individual as the people who have them. It is about making the treatment as individualized as the disease and involves identifying genetic, genomic, molecular, and clinical information that allows accurate predictions to be made about a person's susceptibility of developing disease, the course of disease, and its response to treatment.

The 2003 sequencing of the human genome provided crucial insight into the genetic foundations of countless medical conditions and scientists and physicians are exploiting these foundations to advancing the field of personalized medicine. However, it is not yet an established part of clinical practice, but nevertheless a number of top-tier medical institutions now have personalized medicine programs, and many are actively conducting both basic research and clinical studies in genomic medicine.

Specific advantages that personalized medicine may offer patients and clinicians include:

- Ability to make more informed medical decisions
- Higher probability of desired outcomes thanks to better-targeted therapies

- Reduced probability of negative side effects
- Focus on prevention and prediction of disease rather than reaction to it
- Earlier disease intervention than has been possible in the past
- Reduced healthcare costs

To make personalized medicine a reality, better analytical tools are required to effectively and accurately identify behavior, pathways, and genes that are related to a certain disease in order to assess the patient's risk. Combinatorial analysis of markers, therapeutic drugs, dyes, living organisms, genes is a key to identifying potential personalized treatment. Robotic equipment has been developed to execute such analysis; however, research has been conducted in order to develop alternative systems as current robotic systems are constraint to well-plate footprint at relatively high volumes (microliter range). These systems must fulfill many design constraints, including the capability of multiple cell dispensing, high throughput, effective utilization of reagents, accuracy, and reproducibility of results.

1.4 Miniaturization - the Importance of Screening Volume

In high throughput screening (HTS), higher density lower volume assay plates are being investigated because of the combined effect of decreased reagent/consumable and increased throughput (more assays per plate). For instance, genomics research is pushing toward high density micro-array of DNA. The more DNA 'spots' that can be arrayed per slide, the more genetic variations can be investigated [11]. Current well plates used for routine screening are in the range of 384 - 1,536 wells

utilizing 2.5 - 10 µl of reagents per well as shown in Figure 2. However, some studies have already used 3,456-well plates and total assay volume of 1–2 µl [12], and robotic systems have been developed to accurately and reproducibly pipette volumes as low as 25 nanoliters [13], while the standard 125.76 by 85.48 mm well-plate footprint has been kept. Current trends identified on Figure 2 are: 1) Minimizing reagent volume, 2) increase number of assays per day (throughput), 3) preserving footprint area of the well-plate.

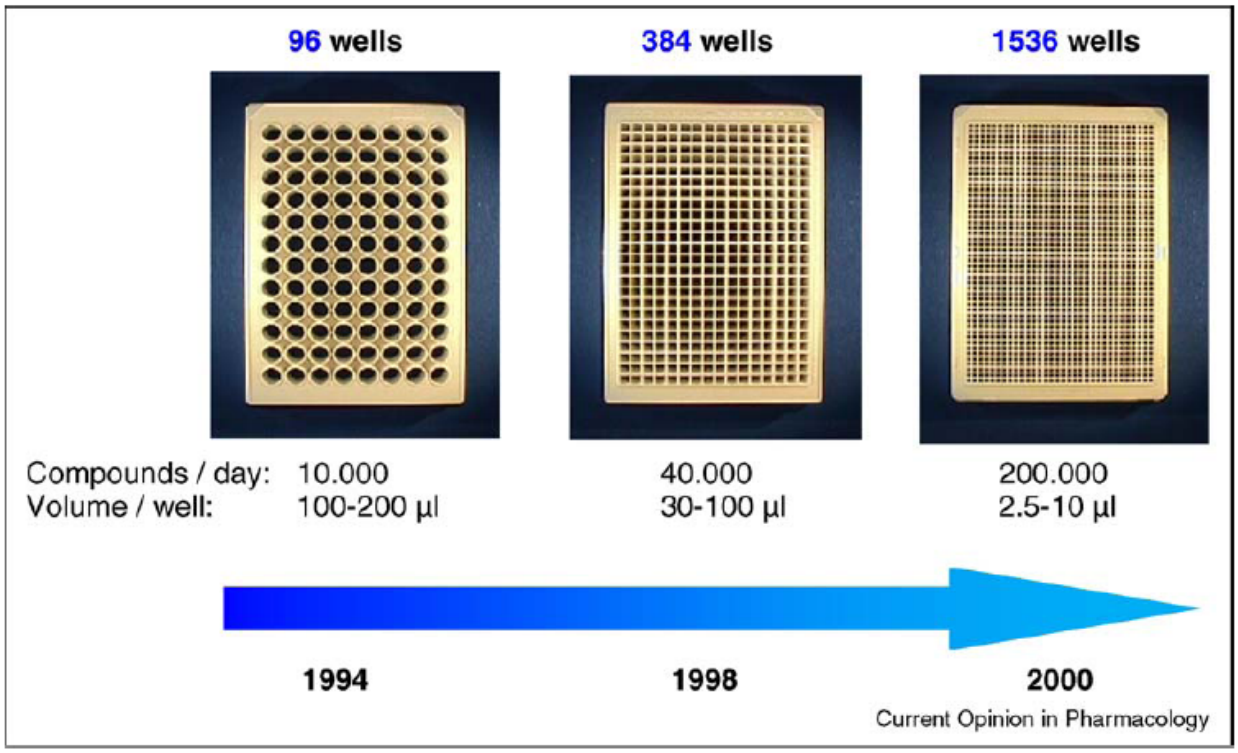

Figure 2. Current trend towards screening miniaturization [14].

CHAPTER 2: LITERATURE REVIEW

2.1 Anticancer Therapy

The conventional approach to cancer therapy has been to provide treatment according to the organ or tissue in which the cancer originates. This approach was appropriate when there was only a rudimentary understanding of the molecular origins of cancer and the different intracellular signaling pathways that are activated in the various types of cancer. In the past two to three decades the genetic events that lead to cancer have been elucidated. It has become clear that cancer develops as a result of multiple genetic defects and that individuals with the same type of cancer often have dissimilar genetic defects in their tumors. These findings explain why patients who seem to have similar cancers respond in a heterogeneous manner to anticancer agents and show the huge obstacle we are faced with to providing effective treatments for cancer. Consequently, cancer therapy has slowly but steadily begun to shift from a ‘one size fits all’ approach to a more personalized approach, in which each patient is treated according to the specific genetic defects in the tumor. Such an individualized approach requires the discovery and development of prognostic biomarkers that help doctors to decide which patients to treat and predictive biomarkers that help in deciding which therapy is most likely to be more effective for a given patient. By definition, prognostic biomarkers predict the clinical outcome for a patient if no anticancer drugs are administered, whereas predictive biomarkers predict the outcome of a specific therapy for a patient. An example of why such biomarkers are needed to improve patient management is that, for some tumors, resection of the primary tumor might be curative;

therefore, systemic therapy to eliminate any remaining tumor cells (also known as adjuvant therapy) would not be needed. By contrast, for more malignant primary tumors, aggressive systemic therapy, often chemotherapy, might be required after resection, in order to reduce the risk of the tumor recurring. However, the distinction between these is often unclear, so prognostic biomarkers that enable the likelihood of recurrence to be determined are urgently needed in the clinic [15].

2.2 Cell Lines and Drugs Background

A recent report by the American Cancer Society (ACS) [16] has summarized the facts of current cancer types affecting the United States. A list of common cancer types includes cancers that are diagnosed with the greatest frequency, excluding non-melanoma skin cancers:

- Bladder Cancer
- Lung Cancer
- Breast Cancer
- Melanoma
- Colon and Rectal Cancer
- Non-Hodgkin Lymphoma
- Endometrial Cancer
- Pancreatic Cancer
- Kidney (Renal Cell) Cancer
- Prostate Cancer

- Leukemia
- Thyroid Cancer

To qualify as a common cancer for the list, the estimated annual incidence for 2012 had to be 40,000 cases or more. Moreover, the following table gives the estimated incidences and mortalities for each common cancer type:

Table 1. Incidence and mortality of common cancer types[17].

Cancer Type	Estimated New Cases	Estimated Deaths
Bladder	73,510	14,880
Breast (Female – Male)	226,870 – 2,190	39,510 – 410
Colon and Rectal (Combined)	143,460	51,690
Endometrial	47,130	8,010
Kidney (Renal Cell) Cancer	59,588	12,484
Leukemia (All Types)	47,150	23,540
Lung (Including Bronchus)	226,160	160,340
Melanoma	76,250	9,180
Non-Hodgkin Lymphoma	70,130	18,940
Pancreatic	43,920	37,390
Prostate	241,740	28,170
Thyroid	56,460	1,780

The top 3 deadly cancer types are lung, colorectal, and breast cancers, while the most incident cancer types are prostate, lung, and breast cancers. As reference some similar statistics from previous years are presented in Appendix A.

2.2.1 Background of Cell Lines Studied

2.2.1.1 Human Hepatocellular Carcinoma Cell Line (HepG2)

Hepatitis B virus (HBV) is the major cause of acute and chronic hepatitis, leading to progressive development of necroinflammatory changes in the liver, which can result in cirrhosis and hepatocellular carcinoma. Although the development of an effective vaccine to prevent HBV infection has shown promising results and should lead to its eventual eradication, antiviral chemotherapy remains the only effective method to prevent the progression of the disease in chronic carriers. Therefore, the development of new antiretroviral agents active against HBV is needed. HepG2 cells have an epithelial morphology and are thought to be a very useful model to study HBV virus replication via transfection. Cells are also used for cancer and apoptosis studies (in particular signaling pathway studies) (from abcam.com)

Hepatocellular carcinoma cells are perpetual, adherent, epithelial-like type cells, which grow as monolayers and in small aggregates. HepG2 cell line was derived from the liver tissue of 15-year-old Caucasian American male with differentiated hepatocellular carcinoma. HepG2 is not tumorigenic in immunocompromised mice. These cells secrete plasma proteins, such as albumin, transferrin, fibrinogen, a-2-macroglobulin, and plasminogen. Cells respond to stimulation with HGH. The vast

amount of studies made with this cancer cell line make it ideal to have more information available for discussion purposes. Doubling time: around 35 hours, from [18]. Figure 3 show a representative image of HepG2 culture in a petri dish.

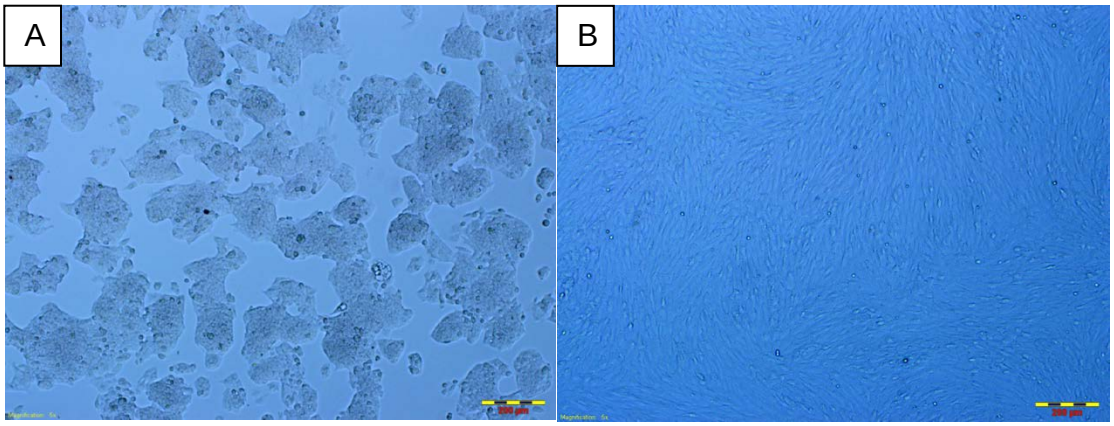

Figure 3. Representative image of HepG2 cancer cells(A) and Epithelial cells (B) in a culture plate.

2.2.1.2 Epithelial Cell Line

Epithelial cells are bound together in sheets of tissue called epithelia. These sheets are held together through several types of interactions, including tight junctions, adherents, desmosomes, and gap junctions (Figure 4).One type of junction found only in epithelium is the tight junction, which is considered by most scientists as the closest junction in the world. Tight junctions act as the delineation between the apical (upper) and basal (lower) regions of an epithelial cell in conjunction with polarization between the two regions. Epithelium is supported on the basal side by a basement membrane called the basal lamina. Below the basal lamina lies the capillary bed, which provides epithelia with required nutrients and disposal of waste products. In addition, the nucleus

in the epithelial cell is usually found closer to the basal surface than the apical surface[19].

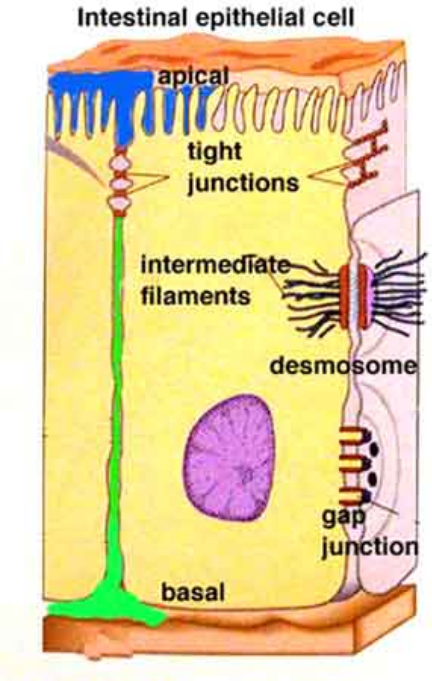

Figure 4. Epithelia are apical to the basement membrane and are characterized by the presence of tigh junctions.

2.2.2 Anticancer drugs

Currently there are many anticancer drugs that are being commercialized for cancer treatments and some others that are under investigation to be applied on clinical therapies. A comprehensive review is given here [20-25]

In general, anticancer drugs have six dosing principles [26-28]:

1. Drugs: more effective in combination (may be synergistic)
2. More effective if drugs do not share common mechanisms of resistance.
3. More beneficial if drugs do not overlap in major toxicities.

4. Drugs should be in administered near their maximum individual doses
5. Drugs should be administered as frequently as possible -- to maximize dose intensity (dose per unit time) limiting tumor regrowth.
6. Desirable: maximum cell kill with each treatment cycle, using the highest dose possible, repeating doses as frequently as tolerable.

These principles have to be in mind while pursuit the development of the current anticancer screening.

2.2.2.1 Cyclophosphamide monohydrate

Cyclophosphamide (cytoxan) is an alkylating agent, a drug that is used primarily for treating several types of cancer. It is used alone or in combination with other medications to treat Hodgkin's lymphoma (Hodgkin's disease) and non-Hodgkin's lymphoma (types of cancer that begin in a type of white blood cells that normally fights infection); cutaneous T-cell lymphoma (CTCL, a group of cancers of the immune system that first appear as skin rashes); multiple myeloma (a type of cancer of the bone marrow); and certain types of leukemia (cancer of the white blood cells), including chronic lymphocytic leukemia (CLL), chronic myelogenous leukemia (CML), acute myeloid leukemia (AML, ANLL), and acute lymphoblastic leukemia (ALL). It is also used to treat retinoblastoma (cancer in the eye), neuroblastoma (a cancer that begins in nerve cells and occurs mainly in children), ovarian cancer (cancer that begins in the female reproductive organs where eggs are formed), and breast cancer. Cyclophosphamide is also used to treat nephrotic syndrome (a disease that is caused by damage to the kidneys) in children whose disease has not improved, has gotten

worse, or has come back after taking other medications or in children who experienced intolerable side effects with other medications [29].

When administrated in vivo, cyclophosphamide first is converted by the liver into two chemicals, acrolein and phosphoramide, which are the active compounds that slow the growth of cancer cells by alkylating DNA. When administrated in vitro, cyclophosphamide interacts with the DNA primarily in site N7 position of guanine (other sites as well). Interaction may involve single strands or both strands (cross linking, due to bifunctional [2 reactive centers] characteristics) Other interactions: these drugs react with carboxyl, sulfhydryl, amino, hydroxyl, and phosphate groups of other cellular constituents. These drugs usually form a reactive intermediate -- ethyleneimonium ion [30]. Unfortunately, normal cells also are affected, and this results in serious side effects. In addition to slowing the growth of cancerous cells, cyclophosphamide also suppresses the immune system and bone marrow, it is referred to as immunosuppressive. The FDA approved Cytoxan in November 1959 [31].

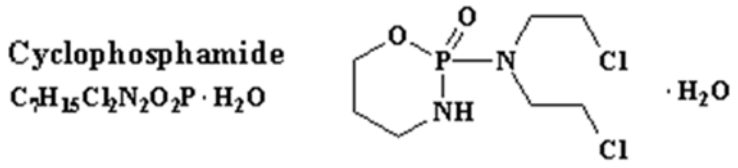

Figure 5. Cyclophosphamide formulation

2.2.2.3 Dichloroacetate Acid

Early investigations focusing in the metabolic differences between cancer and normal cells were made by Otto Warburg, who showed that cancer cells are inherently dependent on glycolysis for production of chemical energy, ATP [32]. A key regulator of cellular metabolism is pyruvate dehydrogenase (PDH), which governs the conversion of pyruvate to acetyl Co-A and therefore, can control the flow of metabolites from glycolysis to the citric acid cycle and subsequently the generation of ATP by mitochondria. PDH is regulated by pyruvate dehydrogenase kinase (PDK) that phosphorylates and inactivates PDH [33]. Dichloroacetate (DCA) inhibits PDK, increasing the flux of pyruvate into the mitochondria, and has recently been proposed as a novel and relatively non-toxic anti-cancer agent [34]. DCA has been shown to reverse the glycolytic phenotype in a number of cancer cell lines, depolarizing the hyperpolarized inner mitochondrial membrane potential to normal levels and increasing mitochondrial metabolism [34, 35]. Because DCA targets a change undergone during tumorogenesis, it can be effective against cancer cells without toxicity to normal cells. DCA is currently in phase III clinical trials for the treatment of chronic lactic acidosis in congenital mitochondrial disorders [36, 37], and thus has the potential to move quickly into the clinic for other applications as it has passed phase I/II toxicity testing in humans [38]. Clinical trials evaluating its toxicity in cancer patients are underway; however, controlled experiments to understand the anti-cancer activities of DCA are needed to determine which tumors and which patients are most appropriate to treat with DCA [39].

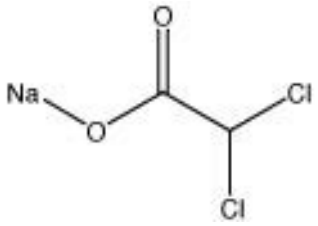

Figure 6. Sodium dichloroacetate molecular structure

2.2.2.4 Solvents

Some agents to be tested have low solubilities in aqueous media, and it may be necessary to use an organic solvent to dissolve them. Ethanol, propylene glycol, and dimethyl sulfoxide have been used for this purpose, but may themselves be toxic to cells. Hence the minimum concentration of solvent should be used to obtain a solution. The agent may be made up at a high concentration in, for example, 100% ethanol, then diluted gradually with balanced saline solution (BSS) and finally diluted into medium. The final concentration of solvent should be <0.5% and a solvent control must be included (i.e., a control with the same final concentration of solvent but without the agent being tested). Care should be taken when using organic solvents with plastics or rubber. It is better to use glass with undiluted solvents and to use plastic only when the solvent concentration is <10%.

2.3 High Throughput Screening (HTS) on Drug Discovery Process

Current drug discovery relies on massive screening of chemical libraries against various extracellular and intracellular molecular targets to find novel chemotypes with the desired mode of action. In recent years, high-throughput technologies for combinatorial and multi-parallel chemical synthesis, automation technologies for the

isolation of natural products, and also availability of large compound collections from commercial sources, have substantially increased the size and diversity of compound collections among most pharmaceutical companies, in some cases exceeding one million distinct chemical entities [14].

The strong increase in both the number of available compounds as well as molecular targets has caused a need for new technological devices able to manage this increase. Various technologies for assay miniaturization, lab automation and robotics have been developed to enable testing of chemical compounds in biological systems High Throughput Screening (HTS) can test 10,000–100,000 per day, and ultra-High Throughput Screening (uHTS) in excess of 100,000 per day [14].

A recent study conducted utilizing gold nanoparticle arrays and chemically detecting cancer biomarker interleukin-6 (IL-6) in serum [40], provided the following detection limits, sensitivity and linear dynamic range for clinical settings[numbers]. This study demonstrated…

Moreover, immunochemical sensing device have been demonstrated useful for pathogen detection in a paper fluidic and inkjet dispensing based approach [41]. Previous work has been done to study inkjet technology as high throughput technology in a bacteria-antibiotic model [42] and enzyme-substrate/inhibitor model[43]. Even though, it has been demonstrated that the inkjet technology is a promising tool for future drug screening at low cost, future evaluation test can be done using different

biomaterials. More targets can be identified for future development of this methodology under the drug screening field.

2.4 Biological Microarray Technologies

Extrusion based robotic systems remain the standard technology used for the liquid handling portion within the high-throughput screening process. Main drawbacks of the current screening process are that they

- Remain time consuming and costly,
- Incur in substantial waste of expensive compounds, plates, disposable tips, and diluents,
- Require high level of expertise,
- Are limited by well-plate footprint, and
- Are prone to cross-contamination

In order to solve these challenges, different approaches have been investigated; many of those improved throughput, lowered test volumes, and increased the density of test wells. A comprehensive review of these technologies, which are classified as contact and non-contact, based on the fluid dispensing mechanism is published elsewhere[7]. Figures 7 and 8 summarize the various technologies and Table 2 discusses advantages and disadvantages of each of those technologies.

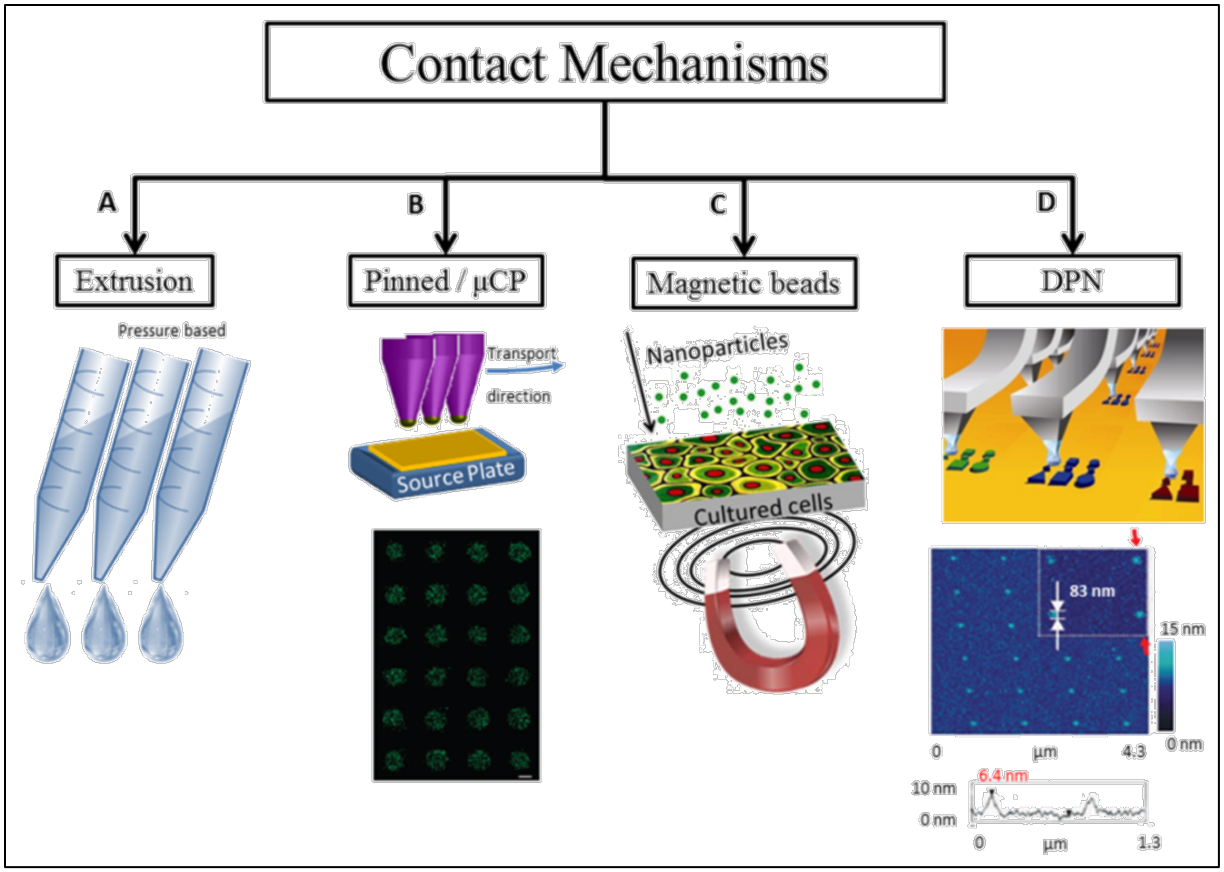

Figure 7. Contact-based technologies for high throughput array construction[7].

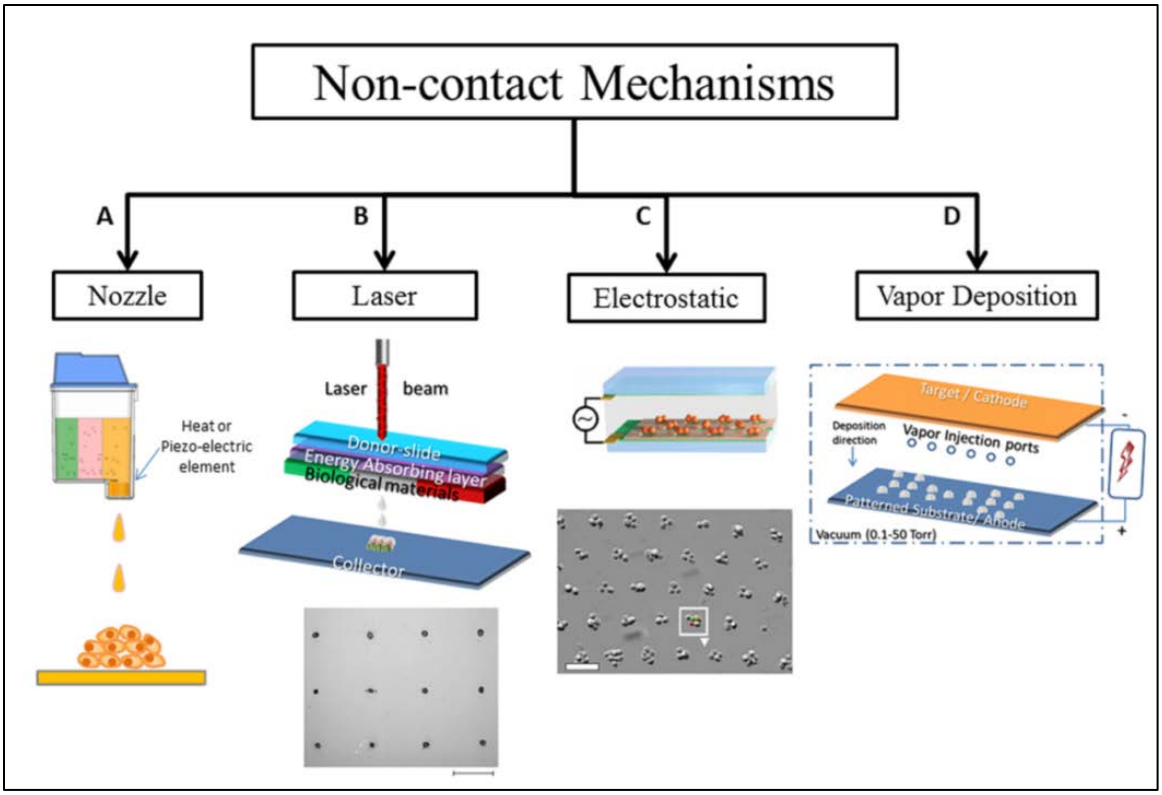

Figure 8. Non-contact based technologies for high throughput array construction[7].

Table 2. Comparison of high throughput assembling techniques[7].

Technology	Advantages	Disadvantages	Resolution/density	Typical applications
Contact methods				
Pinned/micro-contact printing	High density and high precision Easy transfer Less blockages	Need of many pins to meet HT Mechanical stresses due to the physical contact	150–200 μm/ 16 spots/mm^2 [18]	Materials transportation Array construction [11]
Extrusion	Controlled volume Validated technology for decades	Expensive robotic and infrastructure required	2–500 μm [21]/ ~30 k spots/mm^2 (hiScan by Illumina®)	Materials transportation Cell/biomaterials 3-D assembly [14] Sequencing
Magnetic	At-a-distance manipulation High throughput Complex patterns formation	Magnetic nanoparticles may have cytotoxicity Substrate building is time consuming (need to fabricate the die-based substrate)	130 μm/25 spots/mm^2 [38]	Immunoassays [24–26], droplet-based DNA purification [27], active fluid mixing [28]
DPN-AFM	Attoliter scale volume control Nano-resolution and high density	Restricted detection limits Lack of massive multiplexing capabilities [23]	15–100 nm [23, 26]/ 1M spots/mm^2 [23]	Materials transportation Material characterization (e.g., phase separation) [23] Single virus particle control Antibody screening for HIV-1 [83]
Non-contact mechanisms				
Inkjet	Low investment HT Fair precision Picoliter scale volume control Additive operation	Obstruction and blockage Drying and spreading of the ink Limited to low-viscosity materials	15–50 μm/64 spots per mm^2 [50]	Drug screening, biosensing, environmental monitoring, tissue engineering [50]
Laser based	Printing of high-viscosity materials Ultra HT High resolution and density Additive operation	Laser source might have adverse effect on cellular genetic material	1–3 μm [51]/100 spots/ mm^2 [59]	Tissue engineering, cell selection studies, cell-based biosensors, stem cell engineering [51]
Dielectros-phoresis	High precision and high density	Slow throughput DEP forces are inherently transient Substrate building is time consuming (need to fabricate the die-based substrate)	~20 μm / 100 spots/ mm^2 [60]	Cell/biomaterials 3-D assembly, HT arrays, manipulation of biological particles (DNA, viruses, cells) [60, 67]
Molecular volume deposition	Single-cell resolution Complex patterns formation	Unreported throughput Substrate building is time consuming (need to fabricate the die-based substrate)	5–10 μm/100 spots/ mm^2 [72]	Cell-based sensors [84, 85], neurobiology, tissue engineering, patterning on chips (protein, cells) [79]

Among all technologies reviewed, inkjet bioprinting is most promising due to its non-contact capabilities, which can avoid sample cross-contamination, the expandability of cartridges, high throughput, high precision (around 10-50 um), and small volume of reagents dispensed.

2.5 Inkjet Bioprinting

Recently, the inkjet printing technique has attracted much attention as a useful tool for the fabrication of cellular patterns on substrates. In this technique, precise target positions on a substrate can be assigned by computer-assisted deposition. Inexpensive commercially available printers can be used in these experiments with little modification. Several studies have shown the successful creation of cellular patterns mainly on hydrogel substrates by using this inkjet printing technique [44-49]. There are two main strategies, printing with living cells and printing with cell adhesion molecules [50].

Boland and coworkers reported that Chinese hamster ovary cells and primary embryonic hippocampal or cortical cells can be directly printed onto a substrate with a desire pattern without loss of cell function [51, 52]. The printing of cell adhesion molecules such as collagen or cell growth/differentiation factors such as FGF-2 and CNTF with a desired pattern onto a substrate has also been demonstrated using inkjet printers [43, 47-49].

Thermal printers operate by heating of a small air bubble that ejects a drop of ink from the nozzle as it expands. Figure 9 shows a schematic of inkjet bioprinting along zoomed images of micrometer-size nozzles. A typical heating pulse lasts a few

microseconds and drops are fired at a rate of about 5 kHz. For the author, home built systems based on HP head have proven an excellent combination of robustness and cost effectiveness. However, they offer only a narrow window of nozzle voltages and fluid properties in which jetting can be achieved. Therefore ink formulations must fall within a relatively narrow range of viscosities and surface tensions. In addition they have limited tolerance to solvents and strong acids. Customizing cartridges of thermal printers for biological inks is currently being investigated by manufacturers like HP and Olivetti, thus in the future one may be able to use more viscous fluids and avoid the relative large amount of 'dead volume' that is found in current head designs.

Thermal print heads can be mass-produced and are therefore inexpensive and disposable. Most piezoelectric print heads can be cleaned ultrasonically but irreversible damage is still common. Existing thermal inkjet heads are not very solvent resistant and have a limited resistance to acids and bases but bioprinting solutions are mostly aqueous and neutral. While piezoelectric inkjet heads can be solvent and acid resistant, many commercial heads run at high voltages and can be vulnerable to slow degradation in water. In general, thermal inkjet are much more robust than piezoelectric heads in terms of the range of inks that can be printed. The ranges of viscosities and surface tensions of fluids that can be printed are up to 20 cP and 30-40 mN/m respectively. Thermal droplet ejection is a rugged process that is relatively insensitive to other ink properties, as long as some component of the ink can be vaporized. Rheological properties are less important to determine drop formation and jettability, than for piezo-based print heads. Thus even high molecular weight polymers at higher

concentrations may be jettable. There may still be some limitation for biopolymers due to re-filling the ink chamber in the appropriate time to allow for subsequent nozzle firings.

There are several disadvantages of inkjet printing systems over other microfluidic systems; for instance, its resolution of 15-50 μm is lower than other photolithographic and microfluidic techniques. Moreover, this technique is restricted to low viscosity fluids and low cell density to avoid clogging issues [47]. In addition, control of dispensed particles is lost once the liquid has left the confinement of the nozzle, and issues related to drying and spreading of the ink on the surface may render the process less useful. A recent study, however, showed that micropatterned protein spots remained stable on a PEG surface even after extensive washing, demonstrating that the wetting issue can be solved [53]. Further research into ink rheology and fixations properties of bio-inks is needed to lead improvements in resolution, densities, and to minimize clogging issues.

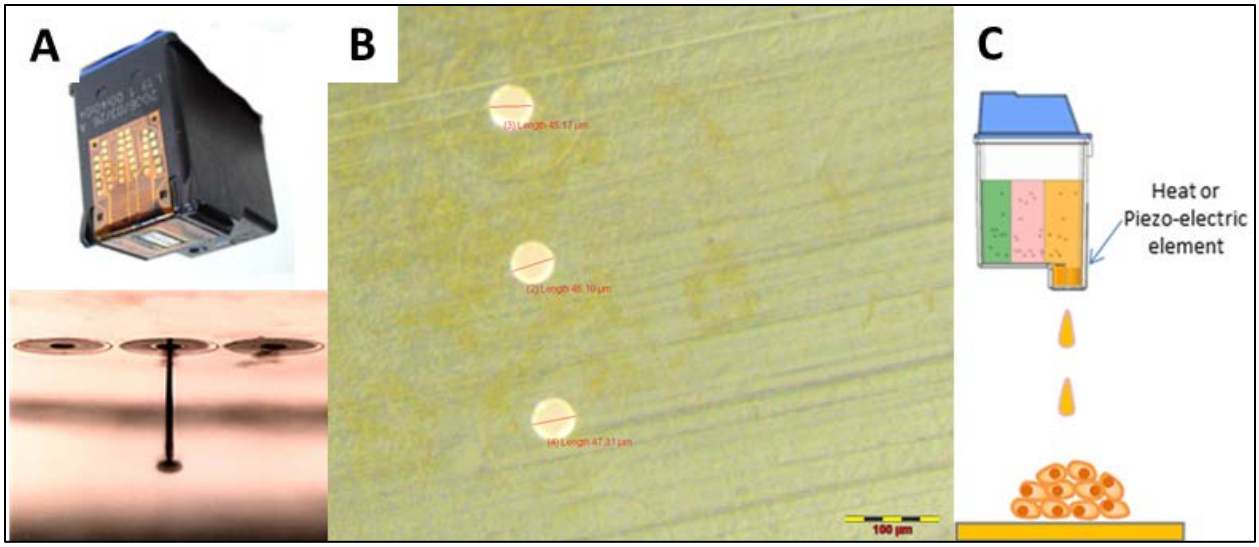

Figure 9. Inkjet technology mechanism. A) Actual inkjet printer cartridge and zoomed image of nozzle actuated to dispensed ink B) Actual picture of cartridge nozzles in research, approximately 50µm in diameter C) Illustration of heater element on side of every nozzle dispensing mammalian cell.

CHAPTER 3: PROJECT RATIONALE

This study is an endeavor to develop a systematic cellomic anticancer drug screening platform based on inkjet printing technology, which will evaluate several anticancer drugs on cancerous and non-cancerous cell lines to identify which treatment and what dosage will be safer and more effective. In particular, a cancerous cell line, HepG2, and a healthy cell line, prostate human epithelial cells (PHEC), have been evaluated under the cytotoxic effect of two chemotherapeutic drugs, cyclophosphamide monohydrate (cytoxan) and dichloroacetate acid (DCA). The screening process is duplicated under the standard micropipetting protocol to ensure that outcomes from the application of inkjet technology fully mimic traditional screening outcomes. Half maximal and 90 percent inhibitory concentrations (IC50, IC90) are obtained from the dose-response curves to correlate both technologies.

The screening platform developed will increase the amount of data obtained from a given sample. The patient's samples -including biopsied cells, saliva, blood, urine, and so on- can be screened at low volume rates along with more targets, thus resulting in less sample usage and more valuable information for an accurate disease diagnosis in the field of medical, environmental, and food analysis. The platform described in this manuscript suggests a change of strategy toward creating a higher density array removing the walls-restricted well-plate approach and minimization of volumes used for an anticancer drug screening.

3.1 Hypothesis

Small quantities of cancer and normal cells can be deposited with and inkjet printer and behave similar to larger, pipetted amounts of cells in terms of growth

Small quantities of two chemotherapy drugs can be precisely added with help of an inkjet printer to standard cell culture plates without losing potency.

3.2 Objectives

a) Standardized miniature platform. Determine minimum dispensable drug volume and associated minimum cell numbers. Determine maximum array density capabilities and fabrication throughput.

b) Verify screening effectiveness with two model drugs and compare against conventional drug screening platform (micro-pipetting). Determine appropriate cell seeding, drug concentrations, survival rates. Develop protocol to minimize time required to obtain outcome results and maximize reutilization of drugs.

CHAPTER 4: HIGH THROUGHPUT MINIATURE DRUG SCREENING PLATFORM USING BIOPRINTING TECHNOLOGY

4.1 Abstract

In the pharmaceutical industry, new drugs are tested to find appropriate compounds for therapeutic purposes for contemporary diseases. Unfortunately, novel developed compounds emerges at expensive prices and current target evaluation processes have limited throughput, increasing cost and time for drug development. The present work shows the development of the novel inkjet-based deposition method for assembling a miniature drug screening platform, which can realistically and inexpensively evaluate biochemical reactions in a picoliter-scale volume at high-throughput rates. Applying a modified Hewlett Packard (HP) model 5360 compact disc (CD) printer, green fluorescent protein (GFP) expressing *Escherichia coli* cells along with alginate gel solution have been arrayed on a coverslip chip under a repeatable volume of 180 ± 26% picoliters per droplet; subsequently, different antibiotics droplets were patterned on top of them, in such a manner that inhibition of bacteria growth was evaluated. The proposed platform was compared to current screening process validating its effectiveness. The viability and basic function of the printed cells were evaluated, resulting in cell viability above 98% and insignificant or no DNA damage on human kidney cells transfected. Based on the reduction of investment and compound volume used by this platform, this technique has potential to improve the actual drug discovery process at its target evaluation stage.

4.2 Introduction

Drug discovery is a time-consuming process and a costly endeavor that requires substantial investment in financial and human resources. It is estimated that more than 800 million dollars over 12-15 years are invested for the development of a single approved new drug [54]. A large portion of the investment is associated with the fact that the new compounds are hard to obtain, particularly in the early stage of development, which drives to expensive research and limited material availability. A cost saving opportunity is foreseeable in the capital invested in fabrication tools for current drug screening platforms. In some cases, a low-cost fabrication tool is of primary consideration, in particular for low resource settings areas. Therefore, low-cost tools and methodologies have to emerge for these underrepresented situations.

Moreover, significant increase in the number of chemical compounds for testing and molecular targets for leading findings can be accommodated only via substantial miniaturization of high-throughput screening (HTS) assays. Applications are driven by the desire to miniaturize processes in order to effectively combine compounds and targets in a rapid manner. In the HTS platforms, higher density at lower volume rate assay plates are pursued to decreased reagents usage and increased throughput. However, most of the existing methods apply a micro- or nano-scale of drug volume at relatively low throughput. In general, the throughput of the current screening processes is limited to 200,000 assays per day at a volume rate of 2.5-100 μl per well [14], which partially satisfies the increasing need of massive screening for future drug development.

To overcome these shortcomings, there is a clear need to develop new technologies to fabricate the next generation of drug screening platform at higher throughput.

Inkjet printing technology offers a possible solution to these issues. This technology is based on the rapid creation and release of liquid droplets, followed by their precise deposition on a substrate. Current commercial inkjet printer generations have reached droplet volumes in the range of 1-95 picoliters (pl), patterning speeds over 250,000 droplets per second [45], and a low-end price in the range of hundreds of USD (United States Dollars). These practical and efficient characteristics to arrayed biomaterials and living organisms [44, 45, 55-57] make this technique suitable for high throughput screening applications. Vast number of studies have used to construct microarrays of biomaterials via extrusion systems [58], laser printing [59-61], direct writing [62-64], thermal and piezoelectric inkjet systems [43, 46, 47, 65-67], microfluidics [68, 69], and other emerging technologies [70-72].

However, to date, only few efforts have been conducted to demonstrate the usage of inkjet technology for drug screening at low volume rates (picoliters range). Such is the case of Arrabito et al. [43] where utilizing a single nozzle piezo-electric printer (Dimatix Materials Printer from Fujifilm, model DMP-2800) biological screening capabilities were demonstrated in a enzymatic inhibitor model. Microarray constructed was proposed to satisfy the requirements of rapid, low-cost, miniaturized (1–10 pL), and HTS (10 spots/s) by easily spotting entire chemical libraries onto solid-supported biological targets. However, incorporation of living organisms (i.e. breast cancer cells, e. coli) is key for drug screening.

For efficient and accurate drug screening purposes, the amount/number of targets (living organisms) should match the dosage of the drug to be tested. Therefore, the HTS system should account for simultaneous deposition of living organisms and drugs in a small volumetric fashion and as post-processing, screening of the cell physiological characteristics under drugs presence will be required. Unfortunately the existing drug screening platforms lack such mechanism and capability. A drug screening platform has been built employing a modified off-the-shelf office inkjet printer that can simultaneously deliver small volumetric amounts of given biochemical substances and corresponding living organism targets to meet the aforementioned needs. This platform can effectively evaluate the behavior of the living organisms in the presence of different drugs (drug screening). In this study we have analyzed the viability and function of the printed bacterial cells by the bacterial live/dead^{TM} assay and plasmid gene transfection experiment. To evaluate its drug screening capabilities, bacteria along with different typical antibiotics were patterned in such a manner that we assessed the bacteria proliferation under three different antibiotics present. Results were compared with manually micro-pipetted samples (most popular method use) containing the same bacteria and antibiotics in order to validate the accuracy of data obtained by the inkjet technology.

4.3 Materials and Methods

4.3.1 Bacterial Strain and Suspension

Escherichia coli (*E. coli*) Efficiency™ DH5α cells (Invitrogen, Stockholm, Sweden) were grown overnight at 37ºC on a Trypticase™ Soy Agar plate (Becton Dickinson & Co, Cockeysville, MD). The bacterial print suspension was prepared according to the protocol we published previously [56]. Briefly, two loopfuls of organisms (representing approximately two large colonies) were transferred into a centrifuge tube containing 5 ml sterilized water. This formed the original print suspension of bacteria. The cell concentration in the *E. coli* solution was determined by the standard plate count method [73]. The tubes containing bacterial suspensions were forcefully shaken before printing, to break up clumps and ensure good distribution of the bacteria. The movement of the cartridge during printing allowed the cells to be maintained in suspension.

4.3.2 Agar Films Preparation

Print substrates were made from soy agar. 7ml of prewarm sterilized BBL™ Trypticase™ Soy Agar solution (Becton Dickinson & Co, Cockeysville, MD) were poured into 100 mm Petri dishes, containing three 24x40mm precleaned sterilized premium cover glasses (Fisher Scientific, Pittsburgh, PA) The solution was allowed to cool at room temperature; when cooled, a thin gel layer was formed on the substrates with a calculated layer thickness of about 1 ± 0.12 mm. This substrate provides the sufficient

nutrients for bacterial proliferation. Agar films were used to evaluate viability of bacteria only.

4.3.3 Viability Evaluation of the Bacterial Array

The viability of the Efficiency™ DH5α cells contained in the printed agar films were evaluated by a two-color fluorescence bacterial live/dead assay (Live/dead® BacLight™ bacterial viability kit, Invitrogen) using a solution consisting of 3.34 mM SYTO 9 in anhydrous Dimethyl sulfoxide (DMSO) 4.67 mM hexidium iodide in anhydrous DMSO (Invitrogen). The samples were viewed using a fluorescent microscope, and the viability of the cells was evaluated by counting the number of cells stained with SYTO 9 (green), and this number was compared to the total number of cells. The viability results of the printed samples were compared to control samples, in which Efficiency™ DH5α cells were manually plated onto a standard tissue culture plate (BD Biosciences, San Jose, CA).

4.3.4 Cell Functionality

The thermal inkjet printing process involves a series of physical interventions including heating (up to 200-300 °C) and mechanical stress (up to 10 ms^{-1}) [47]. To verify if these inkjetting physical interventions could affect the basic properties and functions of the bacterial cells, we examined certain plasmid genes of the printed cells and tested their transfection abilities with mammalian cell line. The pEGFP contained host *E. coli* strain library Efficiency™ DH5α (Fisher Scientific, Pittsburgh, PA) was used for plasmid production. The pEGFP-C1 plasmid was produced and purified in small-

scale using QIAGEN plasmid mini kit (Qiagen Ltd., Hilden, Germany) according to company plasmid purification handbook, 2005. Then it was transfected with human kidney cell line 293 (American Type Culture Collection CRL 1573) using FuGENE® HD Transfection Reagent (Roche, Basel, Switzerland). The culture of human kidney 293 cells was performed according to the vendor's protocol.

Controls were defined as negative when no plasmid was used for human kidney 293 cells transfection, and as positive control when cells were transfected with pEGFP-C1. Two sample groups were evaluated; the first was the plasmid collected from bacteria dispensed by the inkjet printing process and the second was the plasmid collected from bacteria dispensed manually by micropipettes.

4.3.5 High Throughput

An array of points was designed using PowerPoint software (Microsoft Inc., Redmond, WA), formatted under the smallest font size allowed by the software (font size 1), and time was measured from the start of delivery of bacterial cells or drugs until completion of printing. Results were recorded in dots per seconds and the diameter size of the dispensed points was recorded. Typically 41 dots about 420-μm-spaced were dispensed in sequential lines.

4.3.7 Volume Determination

To determine the amount of volume being dispensed by the inkjet printer, an evaluation test was designed to enable theoretical data of volume delivered. Sodium chloride (Acros Organics, Geel, Belgium) and calcium chloride (Acros Organics, Geel, Belgium) were dissolved in distilled water (Millipore, Billerica, MA) in the closest ratio to full saturation, 1:3 and 1:6 respectively. Both solutions were printed with black and color cartridges; and volume was determined by protocol described below.

The procedure for determining the dispensing volume was as follows: a) Clean glass slides were weighed with an analytical balance (model ALF-204, Fisher Scientific, Pittsburgh, PA), b) Different patterns were printed utilizing both solutions (as previously stated) onto clean glass slides to correlate the dot size with the volume dispensed, c) Glass slides with solutions were exposed to 100 ± 15 °C in an oven (Isotemp, Fisher Scientific, Pittsburgh, PA) for at least 10 minutes to allow all the water to evaporate, d) The glass slides, with the remaining salts, were weighed with the analytical balance, e) The printed solution concentration and dot sizes were utilized to determine each volume per dot (Volume (nl) = mass(g) / concentration (g/nl)). However, since the balance had limited precision, arrays and a number of dots were set up in such a manner that a significant difference between the clear and salt-containing glass slides was obtained.

As control, a controlled volume (100 µl) was dispensed over a glass slide under a conventional micropipette deposition method. Percentile errors were obtained from the

test to quantify the tolerance error of the printed parameters under both substances being subjected to the test. Data was recorded and presented in the results section.

4.3.8 Smallest Replicable Volume Dispensed of E. coli

Microsoft PowerPoint software was used to edit a colony array pattern. Three dots in sequential lines under different font sizes (16, 8, 3, 2, and 1) were printed. A black cartridge was emptied of its contents, thoroughly washed, rinsed with a 70% ethanol solution and distilled water, and dried in a sterilized Labculture® Class II, Type A2 Biological Safety Cabinet (ESCO, Hatboro, PA). This cartridge was filled with 1 ml of bacterial suspension (*E. coli* suspended in broth agar) to print a designed pattern. *E. coli* concentration was measured using BioPhotometer plus absorbance reader (Eppendorf, Hamburg, Germany) and the volume calculated from the formula derived in the volume determination section. The *E. coli* suspension was ejected onto an agar coated coverslip and bacterial deposition was read under fluorescent microscope for each dot. Results for cell numbers were plotted, determining the smallest replicable volume being dispensed by the inkjet printing technology.

4.3.9 Drug Screening

To build a single capsule drug screening test and avoid migration by diffusion of the antibiotics and bacteria towards the rest of the deposited dots, three consecutive layers (Figure 10) were printed to encapsulate droplet assays. Over a glass slide, the first printed layer consisted of a solution of sterilized Broth BBL™ Trypticase™ Soy Agar. The second layer consisted of a 0.3% alginic acid solution (Acros Organics, Geel,

Belgium), a liquid known to cross-link under mild conditions to form a biodegradable hydrogel scaffold [74]. Finally, the third layer consisted of an alternating solution of three different antibiotics mixed in a 1:1 ratio to 1.4% Calcium Chloride ($CaCl_2$); all three layers were printed. $CaCl_2$ is known to promote the cross-linking of the individual alginate chains resulting in an encapsulated environment. Black and color cartridges were used as appropiate to take advantage of the four compartments provided by the system employed. The first cartridge (usually containing black ink in 1 compartment) was used to print bacterial suspension, while the second cartridge (usually containing magenta, cyan, and yellow ink in three separated compartments) was used to print three different chosen antibiotics mixed with calcium chloride (1.4% in H_2O). Chosen antiobiotics were penicillin/streptomycin (Fisher scientific), antimycotic (15240-096, Invitrogen), and kanamycin sulfate (15160-054, Invitrogen). Control samples were printed under no antibiotic presence to asses cell population per dot.

Along with the printed samples, micropipeted dots were arrayed on other glass slides, mimicking the drug screening platform proposed at regular volume rates (microliter scale). Results of both proceses were normalized to enable a comparison frame. Normalization was based on the cell population on dots without antibiotics (100 % of the cell population at their distinct volumes), limiting cell population on dots with antibiotics. Results were recorded and plotted. This procedure validates the proposed new inkjet drug screening method.

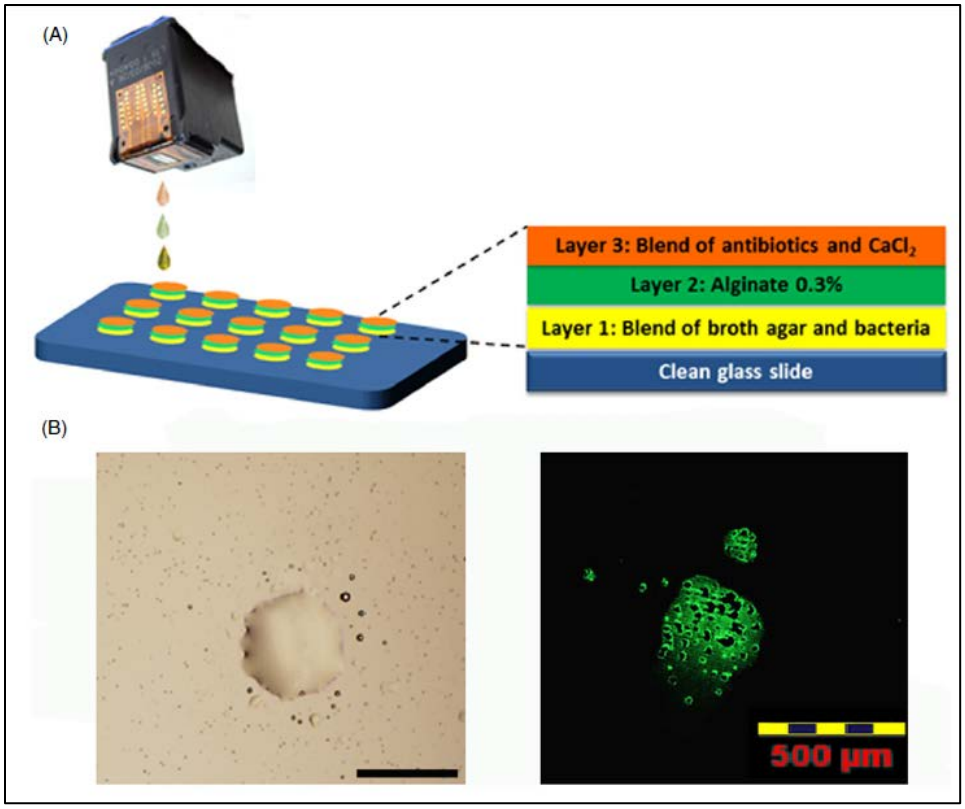

Figure 10. Miniature screening platform. (A) Schematic illustration of the bioprinting process for encapsulating drug-screening droplets on glass slides. (B) Left: representative image of the three layers build of the screening spot. Black scale 500 µm. Right: representative fluorescent image of the screening spot[1].

4.3.10 Image Processing

The technique of selection of similar features on digitized images has previously been employed in previous bioengineering research projects [75-77]. Tone adjustments were made to the original images using the Hue /Saturation tool. The saturation and/or hue of a selected color (using the Eyedropper tools) were modified to i.e. render fluorescent green (live cells) into a more bright green color which separates well from the green background chromogen. Selection of specific color (either fluorescent green or red) in digitized images was used to quantify by means of histogram information

(color pixel numbers, total selected pixel) the amount of living and death cells. This method has been utilized for the quantification of bacteria in the cell viability, functionality, smallest replicable volume dispensed, and drug screening tests.

4.4 Results

4.4.1 Cell Viability

The survival rate of the printed Efficiency™ DH5α cells within the particles was analyzed by a commercial cell survival assay and compared to the controls (n=3), which were prepared by manually placing the cells onto a standard Trypticase™ Soy Agar plate. Printing spots were patterned at three distinct volume sizes: 60, 35 and 7 nanoliters, while control samples were limited to 5 microliters. Percentage of live cells resulted from the test were 99.57 ± 0.108%, 98.81 ± 0.238%, 98.79 ± 0.278%, and 99.66 ± 0.173% respectively. The live/dead assay demonstrated that more than 98% of printed cells remained viable within the microparticles (dots) assessed. After this reading, bacteria was stored in an oven at 37ºC, resulting in exponential proliferation reaching the point that colonies were distinguished by the naked eye.

4.4.2 Cell Functionality

After the transfection test was performed, it was found that animal cells expressed GFP plasmids collected from both sample groups (printed *E. coli* and control sample (micropipetted). Figure 11a and b shows a representative imaging of human kidney 293 cells transfected with the pEGFP plasmids obtained from both groups. The fluorescent expression was evaluated by the image processing method described previously.

Figure 1c shows the percentage of pEGFP expressed in human kidney 293 cells collected from both groups. It was found that both sample groups were significantly equal (p>0.05).

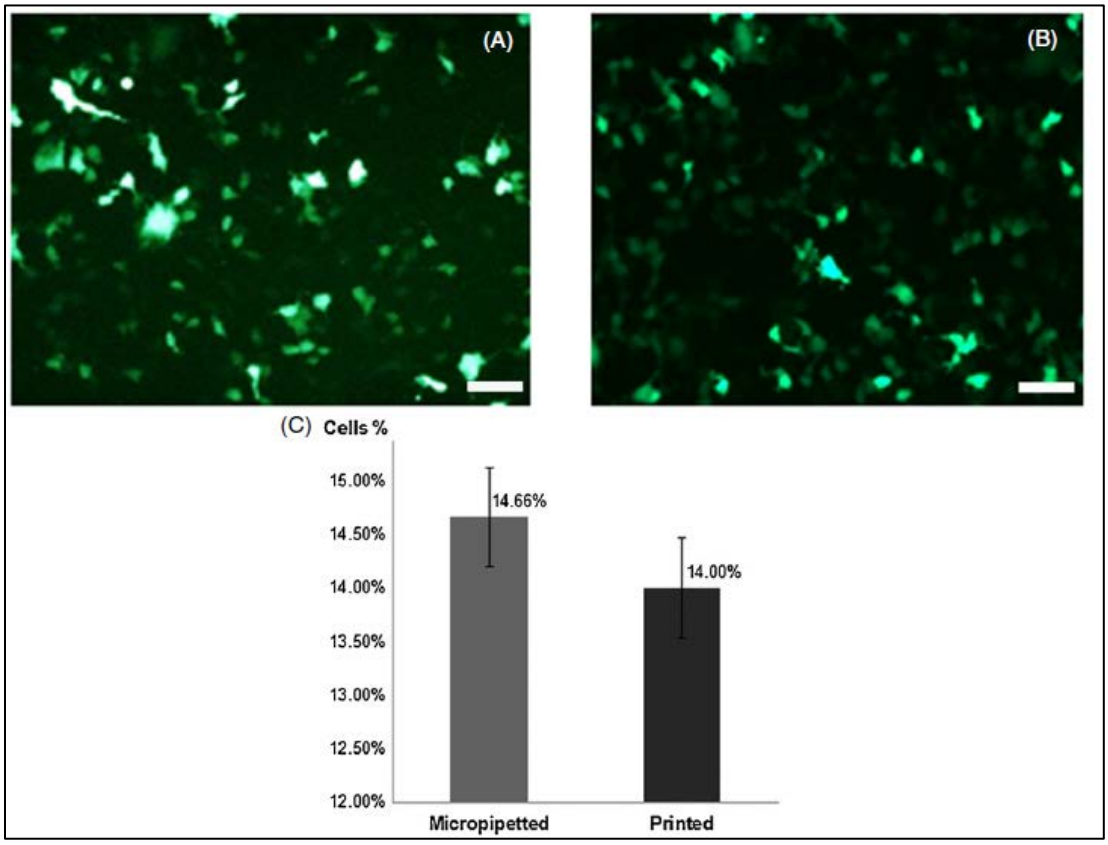

Figure 11. Representative images of human kidney 293 cells transfected with the pEGFP plasmids obtained from the printed bacterial cells (A) and the control (B), a manual micro-pipetted seeding of cells. Percentage of pEGFP expressed on cells collected from manual and print dispensed samples (C). Samples are significantly equal (*p* > 0.05) (*n* = 3). Scale bars for *A* and *B* are 500 *μ*m[1].

4.4.3 High Throughput

This technology has been recorded as a rapid process, which allows for the printing of spots 150–240 µm in diameter at a rate of 213 assays per second, having a theoretical capability of running more than 18 million targets per day.

4.4.4 Volume Determination

Sodium chloride (NaCl) solution was found to be the most reliable substance to be used as a control for the volume determination test, as its percentile error remained below 5 percentile points (4.30 ± 1.66%). On the other hand, calcium chloride ($CaCl_2$) reaches an error of 10.63 ± 1.39%. Therefore, the sodium chloride solution was selected to determine the printing volume in relation to its printing area. Following the procedure explained in the method section, actual data containing the area of the abscissa (x-axis) and the volume of the ordinate (y-axis) was plotted. The actual volume data for deriving this equation was in the range of thousands of picoliters (nanoliters). Different trend lines were drawn, finding a positive correlation within the two sets of data (correlation = 0.99915), which confirms the direct relation between the area and the volume of the printed dots. The polynomial trend line was found to be the best line fit (regression line) (R-squared = 1.0), which resulted in a polynomial equation that describes the behavior of the volume with respect to the printed area. The resulted equation was:

$$volume\ (y) = 3.0789\ area(x)^3 - 20.746\ area(x)^2 + 7643.5\ area(x) + 3\ x\ 10^{-7}$$

This equation was utilized to calculate volume for the bacterial printing sections based on the smaller areas (diameters) of printed dots.

4.4.5 Smallest Reliable Volume Dispensed of E. coli

It is desirable that in every assay the amount of bacteria cells delivered in each dot remain as constant as possible. Figure 12b shows the results of various numbers of

E. coli cells at different font sizes. It was found that the smallest reliable volume was under font size number 3, which dispensed 180 ± 26% picoliters per each colony dot, containing an average cell number of 1,116.7 ± 34.3% (n=3, standard deviation) bacteria cells. Even though the dots exhibited satellite printing spots (Figure 12a), the dispensing area remained fairly controlled. A bacteria spread distribution is visualized in Figure 12c.

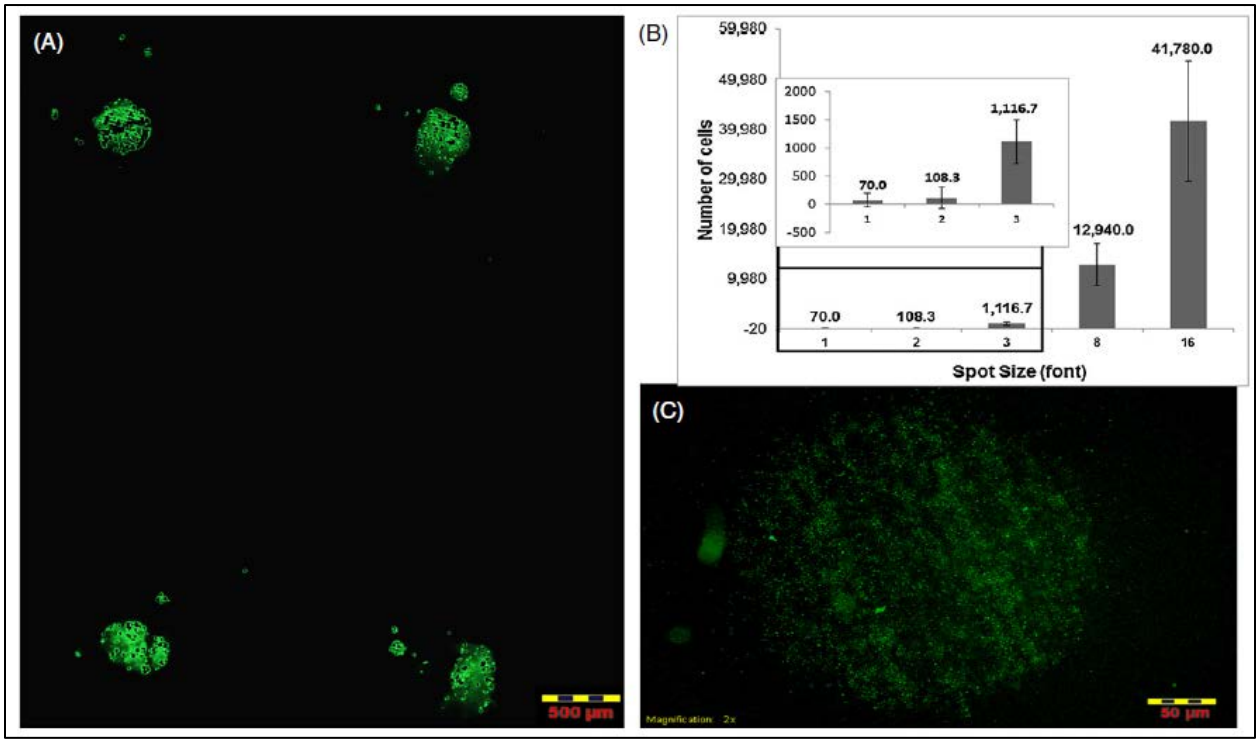

Figure 12. Smallest replicable dots. (A) Array of dots, point size number 3. (B) Number of E. coli strain library Efficiency™ DH5α cells at different font sizes (n = 3). (C) Representative image of smallest replicable dot. Scale bars: 500 µm (A) and 50 µm (C)[1].

4.4.6 Drug Screening

Three bacterial inhibitors were evaluated under the proposed miniature drug screening. Antibiotics included in the test were a penicillin/streptomycin mixture,

antimycotic, and kanamycin sulfate. Figure 13 shows the behavior of the printed microparticles (n=6) comparing *E. coli* under these different antibiotics and under no antibiotics presence as a control. Within the following 10 minutes after printing, the viability test was performed, revealing that the three antibiotics restricted the viability of the cells below the 50% of the control samples (no antibiotic presence). Moreover, to validate if this new method is as effective and efficient as an antibiotic screening method at a low volumetric constraint, it was compared to the manual micro-pipetting methodology. Figure 14 illustrates the normalized plotted data, comparing the *E. coli* expression under different circumstances of both methods. Direct correlation was observed at both methods, demonstrating that the bioprinting method at a low volume setting has similar results to standard micropipetting approach.

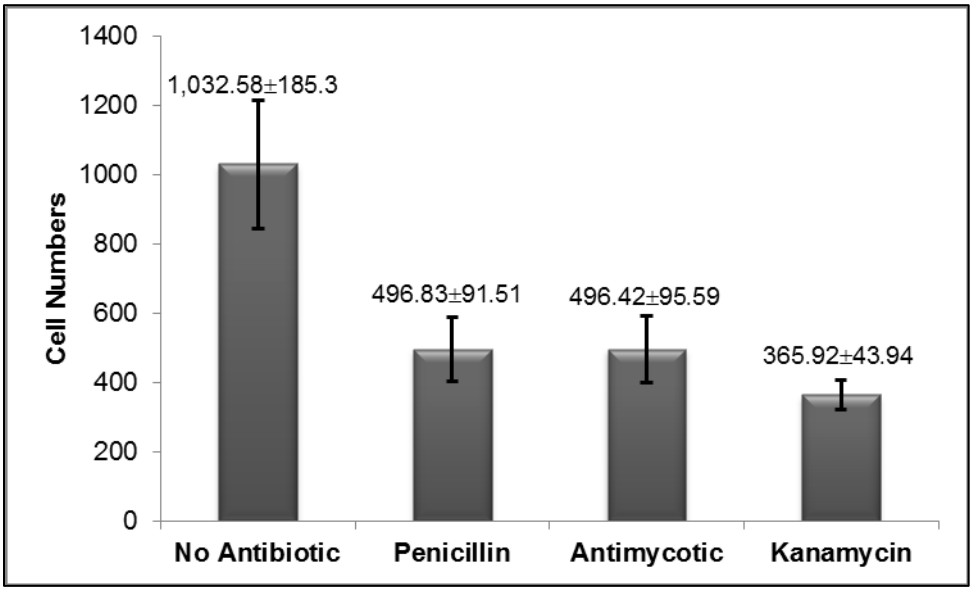

Figure 13. Drug screening of the printed microparticles (n = 6), comparing E. coli under different antibiotics and under no antibiotics presence as a control (data is shown in cell numbers +/− standard deviation)[1].

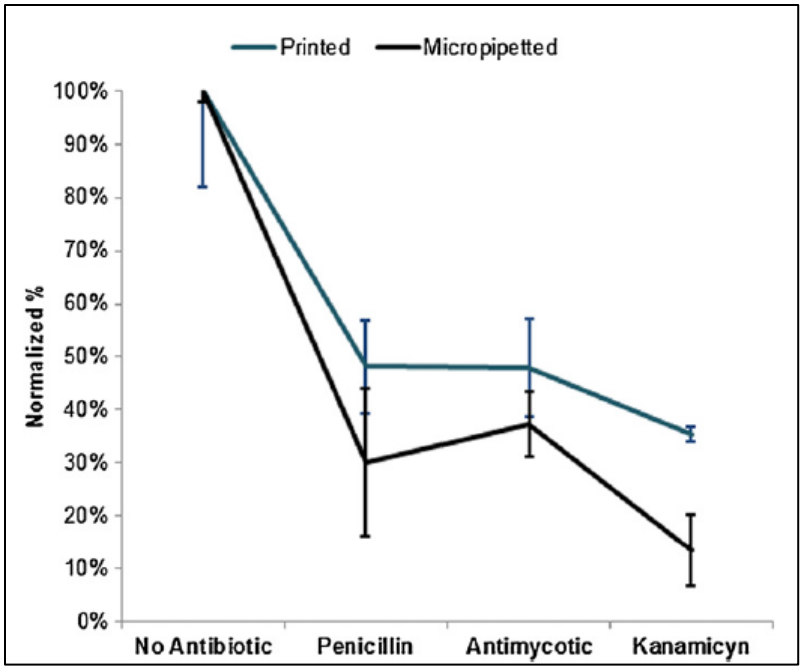

Figure 14. Normalized graph comparing behavior of E. coli under different antibiotics presence by inkjet printed and manually dispensed samples (n = 3)[1].

4.5 Discussion

Drug discovery process has many areas of improvement. While the costly and time-consuming concerns are mostly associated with the pre-clinical and clinical trials there is crucial need on continue on the development of drug titration technologies. The miniature drug screening platform herein described has been developed in an effort to alleviate the money and time investment on these endeavors. The major scientific value of this research stands on the demonstration of the inkjet printing technology benefits to downsizing the volume usage of valuable biochemical substances for drug screening applications at a minimized investment. This advantage clearly fits the mission of pharmaceutical firms. Moreover, developing countries can take advantage of this accessible technology to investigate diseases that are of their particular attention. For

instance, tropical diseases are still common in these countries, the implementation of this platform increases the availability for investigation of such diseases

In this study, living organisms and antibiotics were patterned by inkjet printing technology. The non-contact characteristic of the inkjet technology provides an advantage to maintaining the isolated droplets that were tested. Furthermore, the viability assay verified that this method does not significantly affect the number of viable cells, which supports the hypothesis that this method can be used to effectively deliver living organisms [44]. Moreover, genetic material (GFP plasmid) in the bacteria was not significantly affected by the printing process.

Regarding high throughput, the potential 18 million assays per day denote a well above solution for the current screening limitations [14]. This result locates the inkjet technology above the ultra-high throughput, which corroborates its candidacy to solve the bottleneck associated to the target evaluation within the drug discovery process [78].

In the determination of the volume being dispensed by the inkjet technology, sodium chloride (NaCl) solution was found to be the most accurate substance to be used over the calcium chloride ($CaCl_2$), which can be explained by the fact that the second solution can create strongest bonds with water molecules. However, on top of the error on the measurement method (determined as <5%) concerns exist about the different mechanical properties of the printed bioinks to construct the drug screening platform. This concern is alleviate by the fact that viscosity and surface tension (no data

reported) of all bioinks used in these experiments are not significantly different than the saline solution used to determining the dispensing volume system. Further concerns exist on the exposure of bioinks to heat, in the sense that bioink compositions can be modified during the printing process. Future studies are expected to occur to further understand and solve this type of concerns.

The capability of dispensing 180 ± 26% picoliters per colony dot represents the main advantage of this platform. This work demonstrates that a modified commercial office inkjet printer can deliver living organisms and substances under a small volumetric constrains for drug screening purposes in a chip (plane) design basis. Earlier discovered drugs are launched to the market in expensive presentations to recover their discovery process investment. The miniaturization of the platform herein demonstrated show potential to reduce the resources expenditure in the drug screening processes. To exemplified this resource reduction we can consider that any given chemical used in the screening platform cost 200 USD per µl, while current extrusion robotic systems usually dispense volumes in the range of 0.1-2 µl for each dot assay the 133-226 pl, prove feasible in this manuscript, will reduced the cost per dot assay from 20-400 to 0.026-0.045 USD. On top of that, commercial office inkjet printers (HP, canon, epson) have reach sale values below the 100 USD which overpasses the investment in the range of 10,000-100,000 USD of more sophisticate equipment.

More importantly, in regards to the drug screening results, it can be seen in Fig. 5 that normalized data demonstrates the similarity of both methods along the test sample

groups. This confirms that the inkjet printing technique is an effective method to minimize the typical drug screening test. In particular, the similar composition found in the penicillin/streptomycin mixture and the antimycotic justified the similarity in inhibition results, where even overlapping variance occurs. On the other side, kanamycin sulfate inhibition results between methods differ, suggesting that kanamycin sulfate effectiveness becomes compromised by the implicit heat existed during the inkjet printing process.

4.6 Conclusion

In this research project, it has been demonstrated that this method can effectively deliver replicable cell volume at level of hundreds of picoliters. Due to the reduction of volume, this method will increase the effectiveness of the resources utilized for emerging drug screening processes. Moreover, it was proven that bacteria maintained viability and function after the printing process. Furthermore, different antibiotics can be screened at an ultra-high throughput. The results show promising usage of resources for future ultra-high throughput drug screening through new biochemicals under usage of accessible equipment. The present drug screening method represents a low cost possible solution to stimulate the drug discovering process for developing countries.

CHAPTER 5: COMPARISON OF IC50 AND IC90 BETWEEN MICROPIPETTED AND INKJET PRINTED CHEMOTHERAPY DRUGS ON CELL GROWTH INHIBITION

5.1 Abstract

The new paradigm of personalized medicine is beginning to affect clinical practice. In particular, many of the advances in genomics and proteomics have made personalized screening and therapeutic inventions possible. On chip, cellomics approaches to screening and intervention are becoming more commonplace. Cancer therapies may benefit from the rise in '-omics' technologies. In addition, the availability of rapid screening data is crucial to mitigate cancer propagation and increase the possibility of patient recovery. This study is an endeavor to develop a cellomic anticancer drug screening process based on inkjet printing. Previous research has demonstrated that inkjet based screening can reliably create isolated spots arrays at low volume (180 pl) and high throughput (213 spots/sec). Herein we study whether inkjet printing small volumes of anticancer drugs along with few cells has merit as a tool to fabricate cellomic chips. Cells, from the hepatocellular carcinoma line HepG2 and the epithelial cell line PHEC, were printed with an inkjet device and thus arrayed on a 96-well plate for culture. The inkjet device was described before [1]. At mean exponential proliferation rate, cyclophosphamide monohydrate (Cytoxan) and dichloroacetate sodium (DCA) at standard chemotherapeutic concentrations in the range of 0-50 mM were printed at continuously increasing densities in order to expose cultures to a drug concentration

gradient. Anticancer drugs were studied under two solvents by means of dimethyl sulfoxide and PBS. The printed volumes were in the nanoliter range accounting for 625 ± 20% cells per spot. MTS assay was utilized to determine the amount of viable cells upon 24 hours of drug exposure followed by 48 hours for cell recovery. Half maximal and 90 percent inhibitory concentrations (IC50, IC90) were obtained from the dose-response curve. Along with the proposed cellomic chip, a screening platform using traditional micropipetting technique was built to compare results and validate inkjet based screening platform applicability.

Results obtained show that both cell lines were growth inhibited under both drug regimens. The IC50 values obtained by micropipetting and inkjet based screening varied less than 1mM suggesting that the proposed screening platform closely mimics the traditional screening outcome. However the IC90 values obtained vary in the range of 1 to 4.5 mM. The resulted IC50 indicates that 9.35 and 4.3 mM will be sufficient to inhibit growth of both cell lines under cytoxan and DCA treatment, respectively. In comparison to literature, IC50 results vary based on the cell lines used for the screening platform, but are generally in the range of 4-10 mM. Thus our results are consistent with those that used much larger volumes, validating our hypothesis that screening assays can be further miniaturized.

Inkjet technology shows promise to be used to determine dosages and treatment modalities using the patient's limited supply of biopsied cells. Future expansion of the screening process to more drugs and usage of actual patients' biopsied cancer cells will result in valuable data to forecast efficiency of potential drug therapies.

5.2 Introduction

The new paradigm of personalized medicine is beginning to affect clinical practice. In particular, many of the advances in genomics and proteomics have made personalized screening and therapeutic inventions possible. On chip, cellomics approaches to screening and intervention are becoming more commonplace. Cancer therapies may benefit from the rise in '-omics' technologies. In addition, the availability of rapid screening data is crucial to mitigate cancer propagation and increase the possibility of patient recovery. This study is an endeavor to develop a cellomic anticancer drug screening process based on inkjet printing. Previous research has demonstrated that inkjet based screening can reliably create isolated spots arrays at low volume (180 pl) and high throughput (213 spots/sec)[1]. Herein we study whether inkjet printing small volumes of anticancer drugs along with few cells has merit as a tool to fabricate cellomic chips.

5.3 Materials and Methods

5.3.1 Cell Lines and Culture Conditions

Human hepatocellular carcinoma (HepG2) and prostate human epithelial (PHEC) cell lines were a gift from Dr. Zhang (Biology Faculty Professor at the University of Texas at El Paso). Both cell lines were cultured with Dulbecco's Modified Eagle's medium (DMEM; Gibco BRL, Grand Island, NY, USA) supplemented with 10% fetal bovine serum and 1% penicillin/streptomycin in a humidified atmosphere in 5% CO_2 at 37°C. HepG2 was defined as positive control cell line, which was expected to be growth

inhibit during the screening process; whereas epithelial cell line was proposed as negative control. Due to the increasing need for search of new compounds with cytotoxic activity against cancer cells and mitigated or zero cytotoxicity to the normal cells. Normal cell lines associated with cancer cell lines screened have to be evaluated as well to minimize secondary effects on cancer treatment. Epithelial tissue lines and covers organs and the whole body, among the four main tissue types existing on the body (muscle, connective, nervous, and epithelial tissue), the epithelial cells (EpC) are the most abundant. This abundance makes EpC more susceptible to be affected by cancer growth and its anticancer treatments. EpC were chosen as the expected negative cell line control to evaluate the expected side effects of any given anticancer drug regimen

5.3.2 Printing Suspensions and Printing Systems

Cyclophosphamide monohydrate (AC20396,Fisher scientific) and dichloroacetate acid (DCA) in the form of sodium dichloroacetate (AC33828, Fisher scientific) were dissolved in dimethyl sulfoxide (DMSO) and phosphate-buffer saline (PBS) to a stock concentration of 10 mg per each ml, further dilution was made by adding 10ml of EMEM prior to addition to cell lines. A wide range of concentrations in log increments (e.g., 1 μM–1 mM, and control) were used for first attempt and a narrower range (log or linear) was used based on the results from the first range, for subsequent attempts.

One hundred μl of stock solutions were used to fill a sterilized cartridge (CL-241, Canon). Drug solutions were printed simultaneously using a modified thermal inkjet

printing system (MG2120, Canon). Printer modifications include the override of paper-feeding sensors and removal of printing feeding mechanisms to allow printing over 96-well plates.

5.3.3 Drug Screening Protocol

Cell survival on presence of therapeutic drugs was evaluated via standard microtitration MTS cytotoxic assay [79]. Different 96-well plates were used to compare the conventional method, micro-pipetting, against the inkjet printing method. Assays were triplicated per drug concentration and control sample group. Drug concentrations were prepared up to 10 folds between 5 and 50 mM. Drug exposure was maintained for 24 hours. Half maximal and 90 percent inhibitory concentrations were obtained from dose-response curves. Control samples were defined as follows: positive control: stock drug concentration, and negative control: pure DMSO and PBS, diluted in EMEM for a final concentration below 1%.

Cells in the exponential phase of growth were exposed to the cytotoxic drug. After 24 h exposure, the drugs were removed and the cells are allowed to proliferate for two to three population-doubling times (PDTs) in order to distinguish between cells that remain viable and are capable of proliferation and those that remain viable but cannot proliferate. The number of surviving cells was then determined indirectly by MTS dye reduction. The amount of MTS-formazan produced was determined spectrophotometrically. Please see appendix C for a complete protocol.

In order to investigate if the linear relationship between the MTS assay and small cell numbers found in our system holds true, HepG2 and epithelial cell lines were trypsinized and count using hemocytometer method (Countess® Automated Cell Counter, Invitrogen) using trypan blue staining to distinguish live cells. Different cell densities were prepared from resuspended cell solution to allocated 5,000, 10,000, 50,000, 100,000, and 150,000 cell bodies per well plate in triplicate. Absorbance values at 490nm using ELISA plate reader were obtained after cell cultures were exposed to MTS reagent according to supplier protocol (Promega, CellTiter 96™ AQueous One Solution). Results were plotted and slope was calculated linear regression analysis. The slope relates the cell numbers to the signal provided by spectrophotometer

5.3.4 IC50 and IC90 Studies

Cell density was maintain at 20,000 cells per well and drugs were added after 24 hours, with an inkjet printer. Drugs were printed under stock solution containing 10 mg per ml of both cytoxan and DCA. Ejected volume was control by the inkjet printing system to print all samples in the same round. This process was done approximately in 10 min.

5.4 Results and Discussion

5.4.1 Pre-Screening Studies

Following the MTS supplier recommendation, the linear relationship between cell number and the signal obtained from spectrophotometer was obtained for each cell type used in the drug screening experiments. Figure 15 and 16 shows the plot for the linear

relation between MTS absorbance reading at 490 nm. Higher concentrations were not plotted as they do not fall under the linear phase [79]. Slopes obtained were 27,146 and 37,683 for epithelial and HegG2 cell lines, respectively.

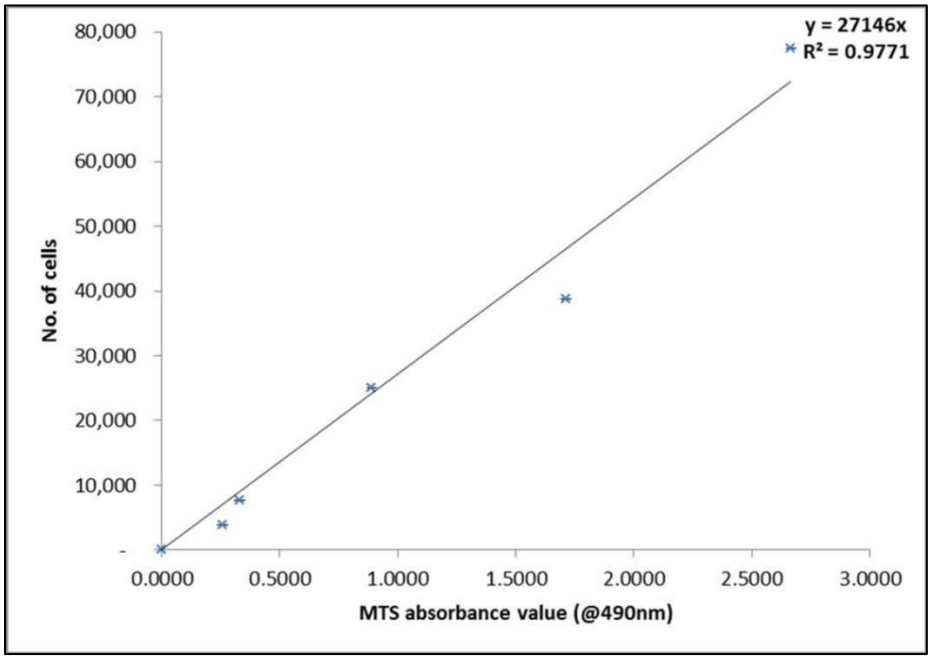

Figure 15. Spectrophotometer signal – Epithelial cell number linear relationship. Top right data shown: slope and r-squared value.

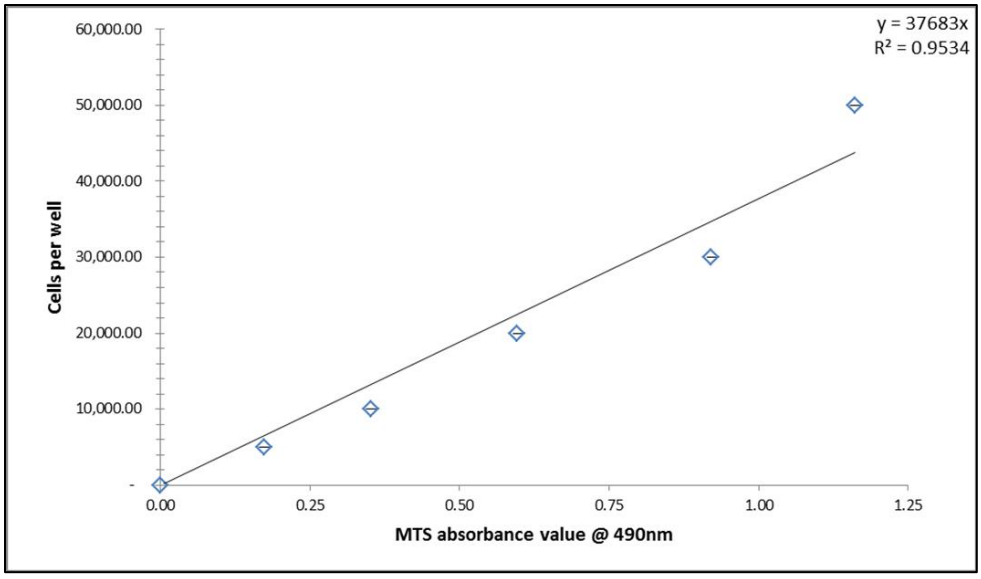

Figure 16. Spectrophotometer signal – HepG2 cell number linear relationship. Top right data shown: slope and r-squared value.

5.4.2 Proliferation Studies for Seeding Stage

A proliferation assay was performed to determine the exponential growth curves of epithelial and HepG2 cell lines. Cell lines were seeded at 5,000, 10,000, 20,000 and 30,000 cells per well. Samples were triplicated and MTS absorbance readings were obtained after 0, 24, 72, 120, 168 and 216 hours of culture. Results for epithelial and HepG2 cell lines are plotted in Figure 17 and 18, respectively. Confluence was observed to be closed to 60,000 cells per well for both cell lines. The drug screening protocol calls for drug exposure during midline of the exponential growth. As seen from the figures, seeding at 5,000 and 30,000 HepG2 cells per well were not good for the drug screening protocol because a lag time was observed, which extends the assay period on one hand, and full confluency was reached too quickly on the other hand. However, seeding at 10,000 and 20,000 cells per well showed that appropriate

proliferating conditions were present. Thus we chose to commence drug exposure at 72 h culture for 10,000 cells per well seeding densities and 36 h for 20,000 cells per well seeding.

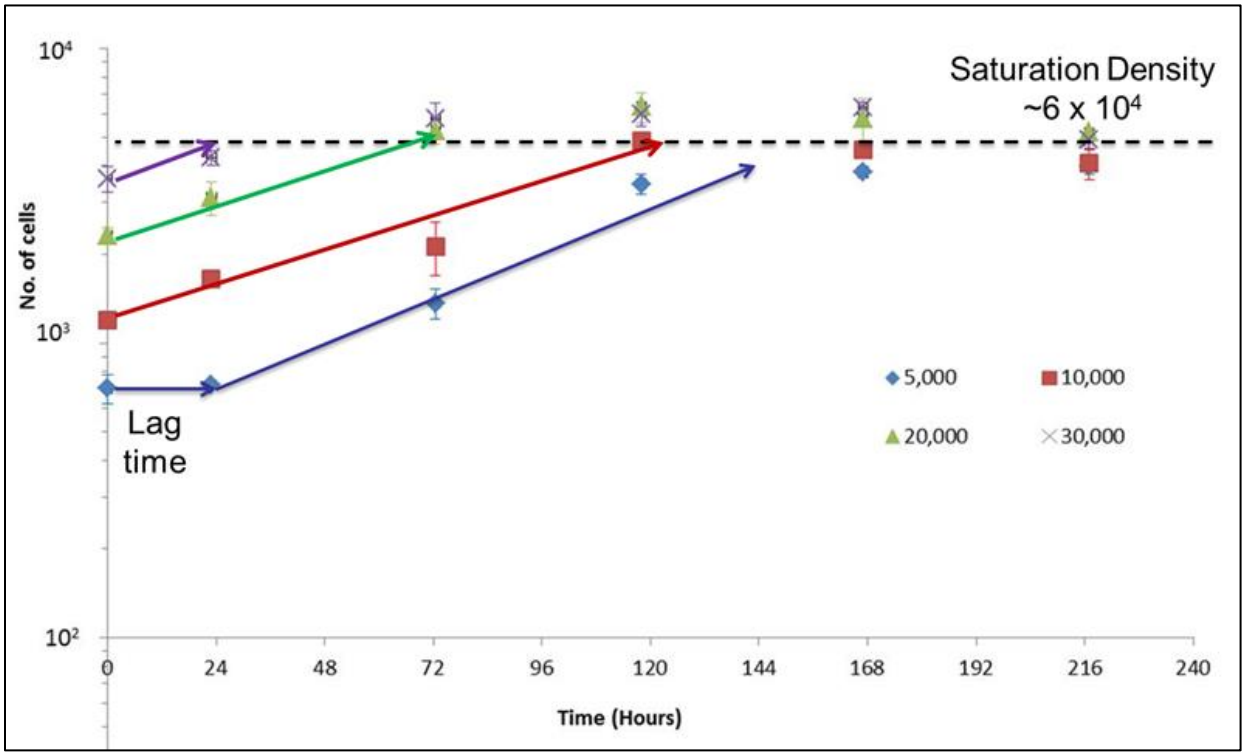

Figure 17. HepG2 semi-log proliferation curves at different cell seeding densities (5,000-30,000 cells per well). n=3

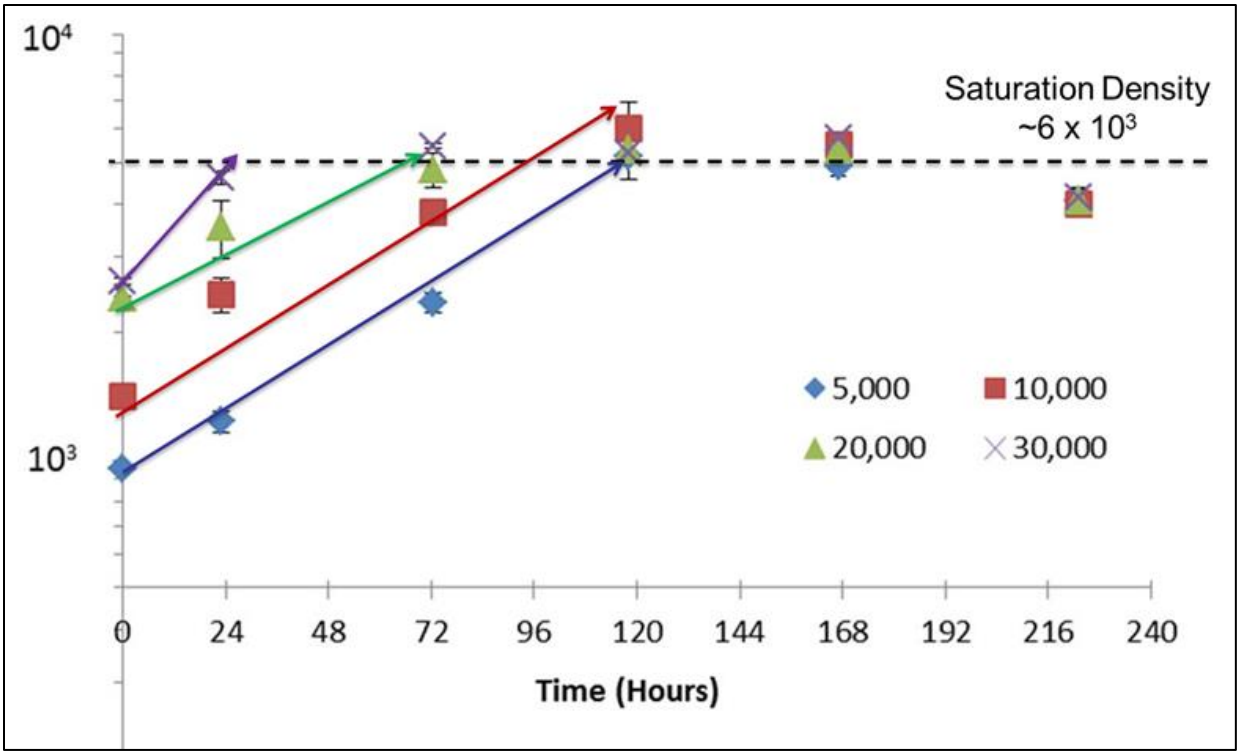

Figure 18. Epithelial semi-log proliferation curves at different cell seeding densities (5,000-30,000 cells per well). n=3

5.4.3 IC 50 and IC 90 Studies using Micropipetting Technique

The survival fraction plotted in Figure 19 show that each drug regimen had similar effect on both cell lines. Drugs were dissolved in DMSO as study reported in appendix D found it more suitable for the screening process. Higher concentration of cytoxan was required to inhibit growth than DCA. When exposed to cytoxan IC50 for HepG2 and EpC was approximately 8.7 mM. When exposed to DCA IC50s were 5 and 4.35 for HepG2 and EpC, respectively. Observing the 90 percent inhibitory concentrations, IC90s were identified as 6mM when exposed to DCA and 11.5 mM when exposed to Cytoxan.

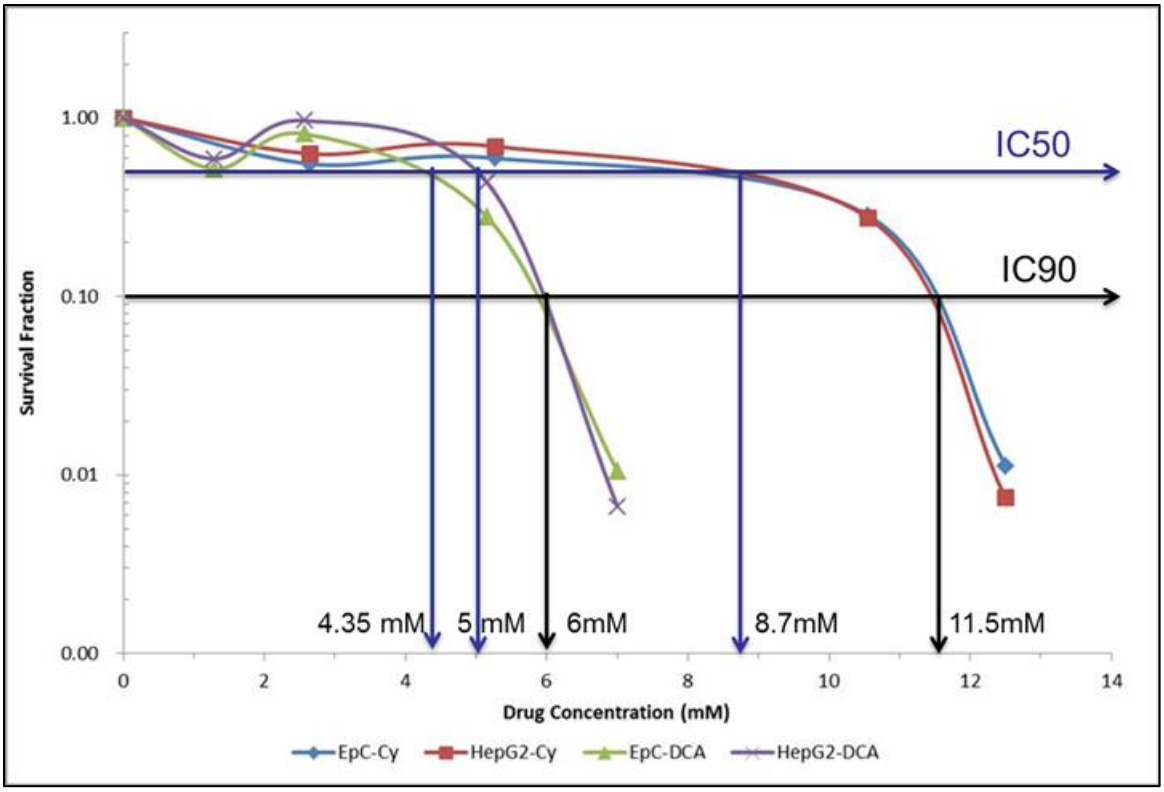

Figure 19. Dose-response curves by micropipetting technique. Survival fraction of epithelial and HepG2 cell lines under cytoxan and dichloroacetate treatment at increasing concentrations when diluted in dimethyl sulfate oxide (DMSO). n=3. Identification of half maximal and 90% inhibitory concentrations (IC50 and IC90)

5.4.4 IC 50 and IC 90 Studies using Inkjet Printer

Initial drug stock concentrations were printed simultaneously using printer system described before. Data resulted is reported in Appendix E. A clogging issue was presented and as result new cartridges were used for each group sample to avoid it. Figure 20 shows the inhibitory effect of the drugs printed at varying concentrations. Cytoxan had same IC50 and IC90 for both cell lines, namely 9.35 and 15.65 mM, respectively. DCA, in the other side, showed small differences of IC50 and IC90

between cell lines. Its IC50 for epithelial cell line was 4.25 mM and for HepG2 4.75 mM. While the IC90 for epithelial was 7mM and for HepG2 7.625 mM.

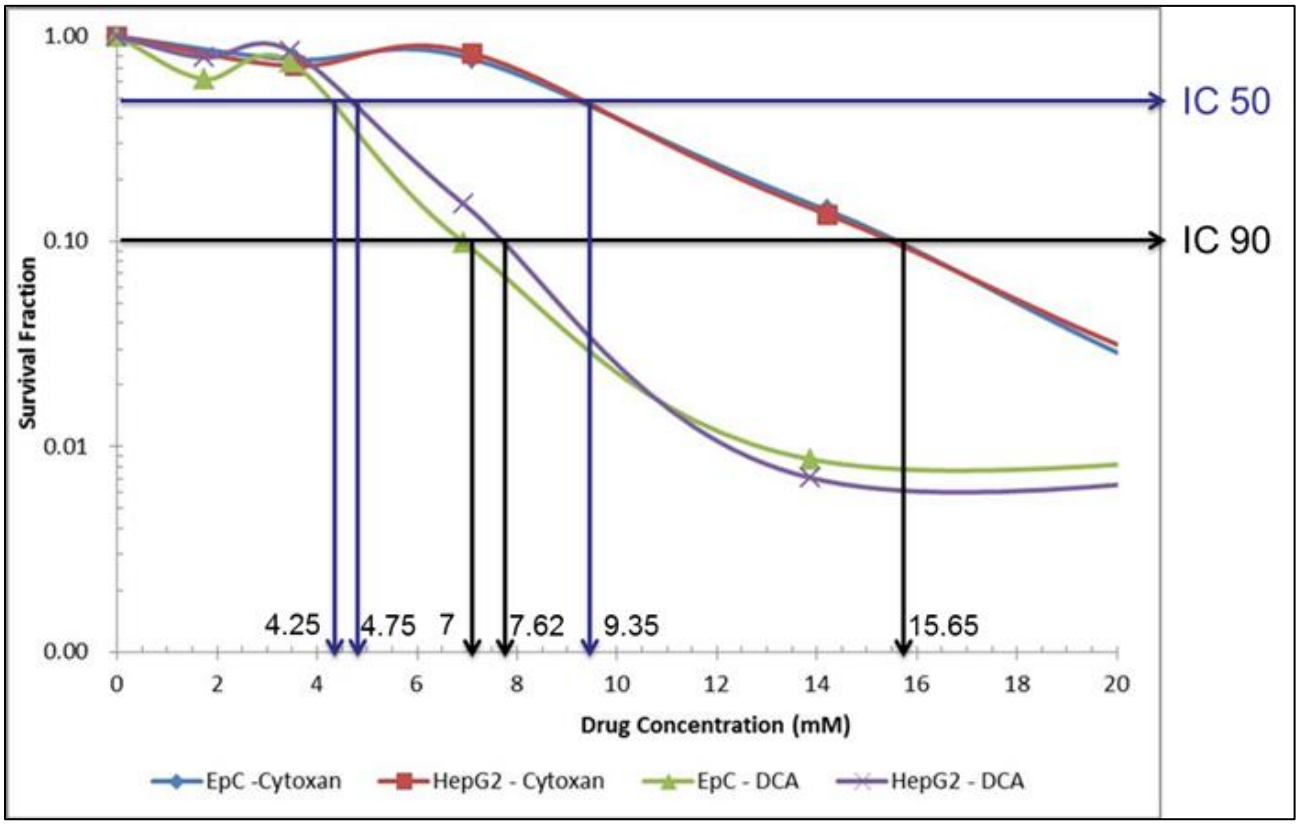

Figure 20. Dose-response curves by inkjet printing technique. Survival fraction of epithelial and HepG2 cell lines under cytoxan and dichloroacetate treatment at increasing concentrations when diluted in dimethyl sulfate oxide (DMSO). n=3. Identification of half maximal and 90% inhibitory concentrations (IC50 and IC90).

5.4.5 Discussion

Applying a modified inkjet printer, cancer cells along with anticancer drugs were arrayed on a 96-well plate in such a manner that inhibition of cancer cell growth was evaluated under various drug concentrations. The proposed platform was comparable to standard micropipetting based screening processes.

On the other hand, personalized medicine promises to refine diagnosis, guide optimum treatment, and avoid unnecessary side effects. In the personalized medicine protocol, study of patient's cells is often needed. In particular, biopsied cancer cells can be analyzed in an *in vitro* anticancer drug screening test to determine the appropriate dosage and drug for those particular cells. To this purpose, this specific screening platform should have several critical requirements, such as capability of multiple cell dispensing, high-throughput, effective utilization of reagents, accuracy, etc. Inkjet printing technology shows promising for fulfilling these requirements

Cancer chemotherapeutic drugs are often administered at their maximum tolerated doses (MTD) to maximize the killing of malignant cells; however, the effectiveness of this approach is limited by the collateral damage to proliferating cells in the intestinal epithelium, bone marrow, and hair follicles [80]. Strategies similar to the one presented can improved these side effects by better relating the most appropriate dosage.

5.4.5.1 ICs across technologies

Table 3 shows a summary of the inhibitory concentrations obtained. It can be seen that the IC50 concentrations are identical within uncertainty ($p > 0.05$) across technologies.. When comparing with literature reports, Sun et al [39] reported that around 5mM of DCA are sufficient to inhibit 50% of the cell proliferation. Figures 21 and 22 show a correlation plot between inkjet based and micropipetted IC 50's and IC90's.

This result indicates that inkjet printing has potential to minimize screening processes and result on similar outcomes as those elicited by higher-volumes assays

Table 3. Summary of inhibitory concentrations at 50 and 90 percent obtained by micropipetting and inkjet printing technique.

		Micropipetting		Inkjet Printing		Delta (Δ)	
Drug	Cell Line	IC50 (mM)	IC90 (mM)	IC50 (mM)	IC90 (mM)	IC50 (mM)	IC90 (mM)
Cytoxan	EpC	8.7	11.5	9.35	15.65	0.65	4.15
	HepG2	8.7	11.5	9.35	15.65	0.65	4.15
DCA	EpC	4.35	6	4.25	7	0.10	1
	HepG2	5	6	4.75	7.625	0.65	1.625

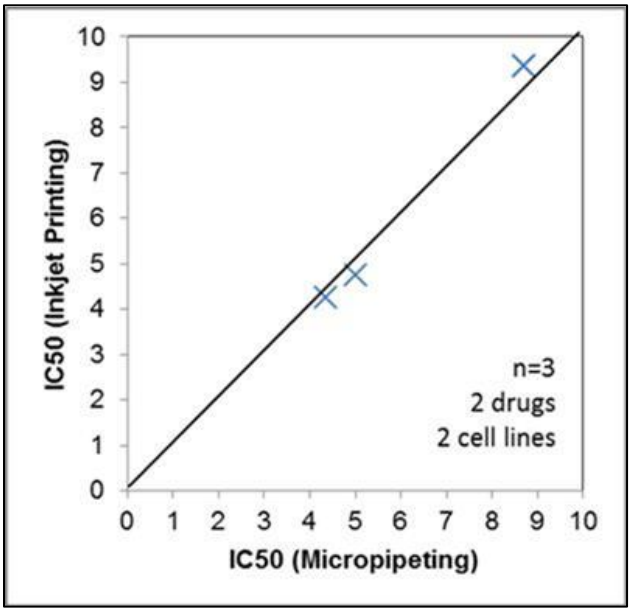

Figure 21. Correlation plot for half maximal inhibitory concentrations comparing inkjet printing and manual micropipetting techniques.

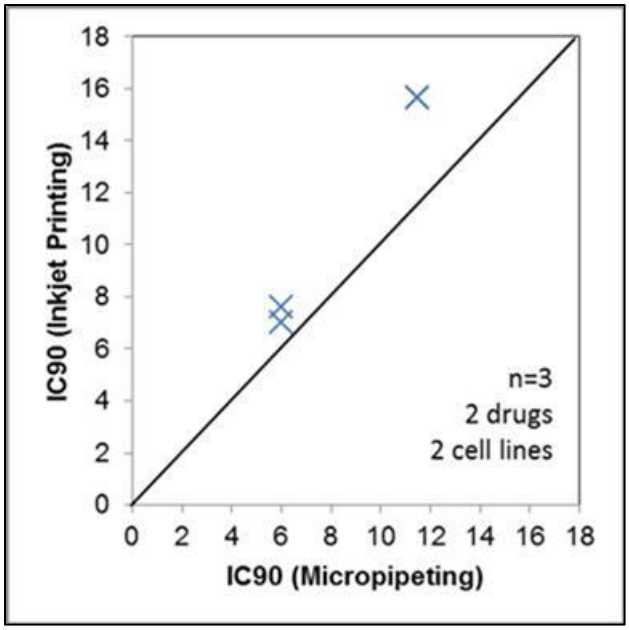

Figure 22. Correlation plot for 90% inhibitory concentrations comparing inkjet printing and manual micropipetting techniques.

5.4.6 Screening Process Optimization

Traditional screening process consists of many steps for the preparation of the series of drug dilution, including drug dilution in solvents for stock concentration, preparation of centrifugal tubes, drug serial dilution for desired concentration, secondary dilution on culturing medium, to later duplicate, triplicate, or quadruplicate samples, plus within the whole process is necessary to maintain suspensions homogeneous to avoid precipitations. While robotic systems have been designed to help this biological task, there are many disadvantages such as accumulated pipetting error, carryover, edge effects, excessive use of disposable materials (tips, centrifugal tubes) and relative high volume consumption.

Inkjet printing system can alleviate issues aforementioned by a part of time expend on preparing the required drug concentrations. Drug stock concentration was loaded into the inkjet-headed cartridge and the highly precise volume control enables the system to directly dispense the replicates and create immediate blends and/or combinations to expedite the screening process. A set up time is required when direct inkjet printing is initially implemented but for further trials the same set up can be utilize.

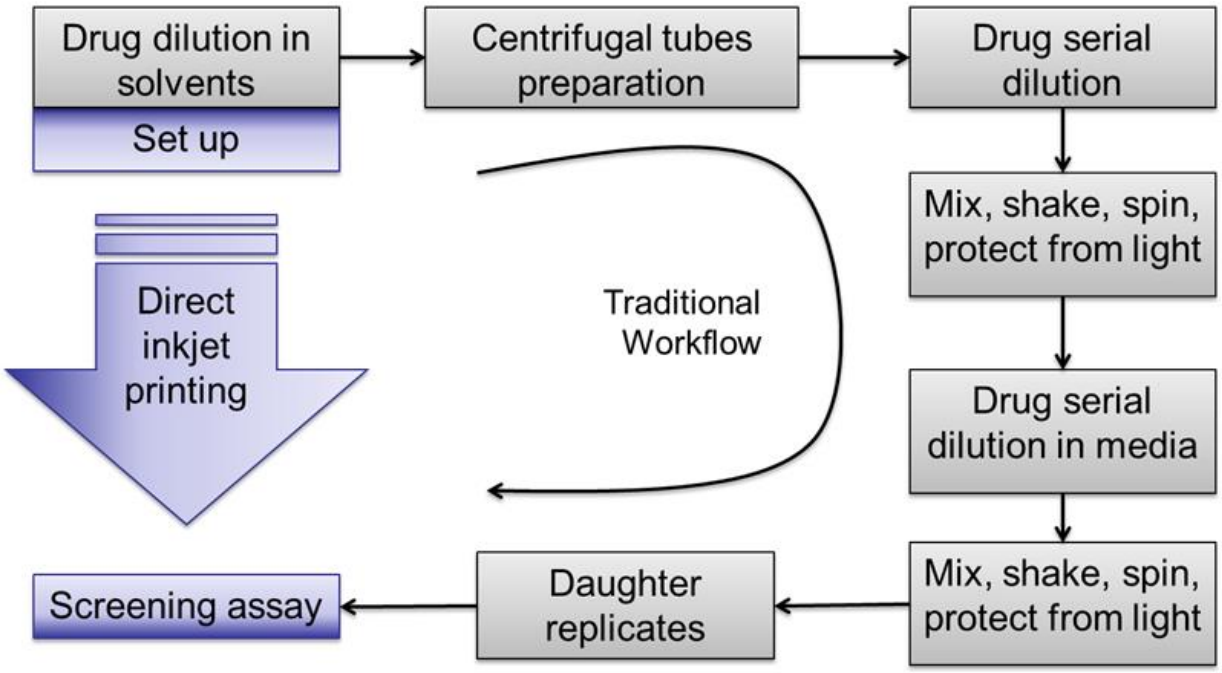

Figure 23. Schematic of drug screening process comparing traditional workflow and proposed direct inkjet printing.

5.5 Conclusions

Results obtained show that both cell lines were growth inhibited under both drug regimens. The IC50 values obtained by micropipetting and inkjet based screening

varied less than 1mM suggesting that the proposed screening platform closely mimics the traditional screening outcome. However the IC90 values obtained vary in the range of 1 to 4.5 mM. The resulted IC50 indicates that 9.35 and 4.3 mM will be sufficient to inhibit growth of both cell lines under cytoxan and DCA treatment, respectively. In comparison to literature, IC50 results vary based on the cell lines used for the screening platform, but are generally in the range of 4-10 mM. Thus our results are consistent with those that used much larger volumes, validating our hypothesis that screening assays can be further miniaturized.

Inkjet technology shows promise to be used to determine dosages and treatment modalities using the patient's limited supply of biopsied cells. Expansion of the screening process to more drugs and usage of actual patients' biopsied cancer cells will result in valuable data to forecast efficiency of potential drug therapies

CHAPTER 6: PROLIFERATION OF HUMAN CELL LINES ARRAYED VIA MODIFIED OFFICE INKJET PRINTING SYSTEMS

6.1 Abstract

Modified office inkjet printing systems have been recently introduced into bioengineering applications demonstrating that it can precisely deposit viable biological molecules, including DNA and mammalian cells. However, further characterization of these cells after printing is required. The goal of this study was to characterize the proliferation of curves of printed cells with different printing systems to understand the process effect over cell ability to proliferate. In particular, using modified Hewlett Packard (HP) 340 and 690 models and their respective cartridges, human cell lines, HepG2 and epithelial cells suspended in phosphate buffered saline (PBS) were dispensed over 96-well plates filled with culturing medium (EMEM). Proliferation curves were evaluated over the period of 12 days using tetrazolium compound assay (MTS). After printing, the appearance of both cell lines on the 96-well plate show regular cell morphology suggesting that printing system did not affect the cell health. Cell confluency was achieved by the seventh day after culturing for HepG2 and epithelial cells. These results suggest that mammalian cells can be effectively delivered by a modified thermal inkjet printer onto biological-compatible substrates at high throughput rate. Inkjet printing technology holds potential for creating high density arrays of living organism in an attempt to build faster and lower volume cell-based screening experiments.

6.2 Introduction

Recently, the inkjet printing technique has attracted much attention as a useful tool for the fabrication of cellular patterns on substrates. In this technique, precise target positions on a substrate can be assigned by computer-assisted deposition. Inexpensive commercially available printers can be used in these experiments with little modification. Several studies have shown the successful creation of cellular patterns mainly on hydrogel substrates by using this inkjet printing technique [44-49]. There are two main strategies, printing with living cells and printing with cell adhesion molecules [50]. Boland and coworkers reported that Chinese hamster ovary cells and primary embryonic hippocampal or cortical cells can be directly printed onto a substrate with a desire pattern without loss of cell function [51, 52]. The printing of cell adhesion molecules such as collagen or cell growth/differentiation factors such as FGF-2 and CNTF with a desired pattern onto a substrate has also been demonstrated using inkjet printers [43, 47-49].

Inkjet printing is a non-contact reprographic technique that takes digital data from a computer representing an image or character, and reproduces it onto a substrate using ink drops [81]. The inkjet technology has been successfully adapted to medicine and biomedical engineering applications, such as drug screening, genomics, and biosensors [82-84]. Herein we study the proliferation behavior of cancerous and non-cancerous cells when dispensed at low volume rates with a modified office inkjet printer.

6.3 Materials and Methods

6.3.1 Printing Suspensions Preparation

Two cell lines were prepared including human hepatocellular carcinoma HepG2 and epithelial cell lines. One plate per cell line was trypsinized when plate confluence reach 80% approximately. Cell pellets were collected by centrifugation (1000 rpm for 5 minutes) in a centrifugal tube. After aspirating supernatant, cells were resuspended in Dulbecco's phosphate buffered saline solution (DPBS) (Sigma Chemical Inc., St. Louis, MO) to obtain cell printing suspensions. The concentration of the cell's printing suspension were measured through hemocytometer method using trypan blue staining [85], cell density was kept at rate of 1,000,000 cells/ml. Cell suspensions were strained at 40 µm to avoid agglomerations and minimize clogging of inkjet cartridge. The tubes containing suspensions were shaken before printing, to break up clumps and ensure good distribution. The movement of the cartridge during printing helps the cells to be maintained mix heterogeneous. Cell suspensions prepared were added in a sterilized cartridge and cells were dispensed at low volumetric constrains in the range of 200 to 1,000 nanoliters. Cells were manually count with the inverted microscope.

6.3.2 Inkjet Bioprinting Set up and Proliferation

HP DeskJet 340 and 690 printers and HP cartridges HP26 and HP29 were modified with the use of the methods previously described [44]. Cartridges were filled with 100 µl of cell printing suspensions previously prepared upon printing into 96-well plate containing 375 µl of EMEM. Group samples were arrayed in duplicate to measure

cell proliferation using MTS assays up to 12 days (188 hrs). Absorbance values at 490nm using ELISA plate reader were obtained after cell cultures were exposed to MTS reagent according to supplier protocol (Promega, CellTiter 96™ AQueous One Solution) for every other day to record proliferation curve.

6.3.3 Results and Discussion

Figure 24 shows the number of cells as function of printing volumes dispensed by the inkjet system. It can be seen that the variation on the number of cells increases as the volume being dispense increase. In the same way, it is observed that inkjet printing systems have a more reliable quantity as volumes diminishes.

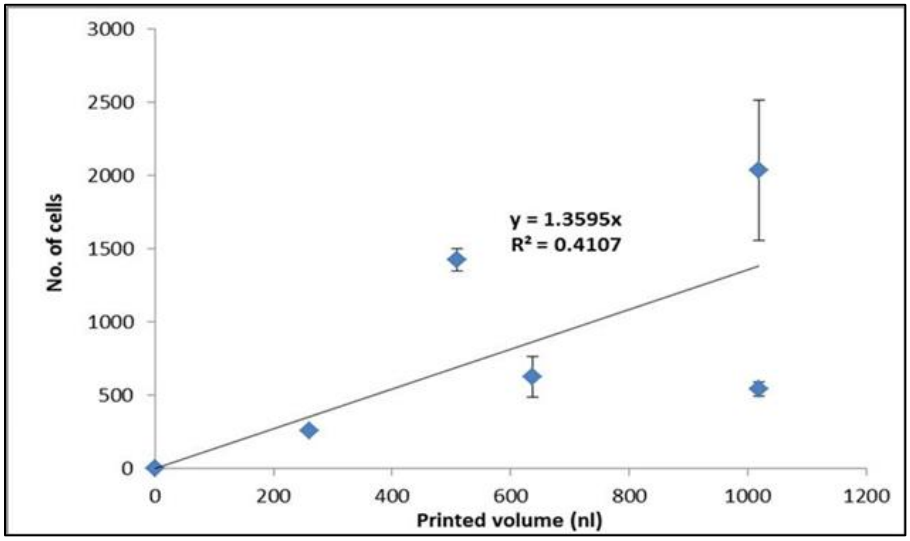

Figure 24. Number of cell bodies (epithelial cell line) per printed volume. n=6

We also investigated different inkjet printing system in order to utilize the most appropriate system for cell seeding. HP 340 and HP 690 were used to eject epithelial and HepG2 cell suspensions. A set of two samples per each day were seeded for a

total of 12 samples. The cells were allowed to proliferate and growth curves are shown in Figure 25 for epithelial cells and Figure 26 for HepG2. Both cell lines were printed at same rates and as result proliferation behavior observed was different. In the case of epithelial cells (Fig. 25) were used to compare the 340 and 690 printer systems. It was observed that cells printed with the 340 printed system reach well confluency earlier, around 168 hours, that the ones printed with the 690 system, around 288 hours. There was no significant difference ($p<0.05$) across seeding volume for each printer system used, suggesting that at this small volume cell growth overcomes printing volume difference. On the other hand, printed HepG2 had a longer lag period ranging from 120 to 168 hours after seeding. In this case, higher volume printed (1,016 nl) was able to reach confluency, however was not the same case for the lower volume printed (508 nl) which even after 264 hour of cultivation was not able to growth.

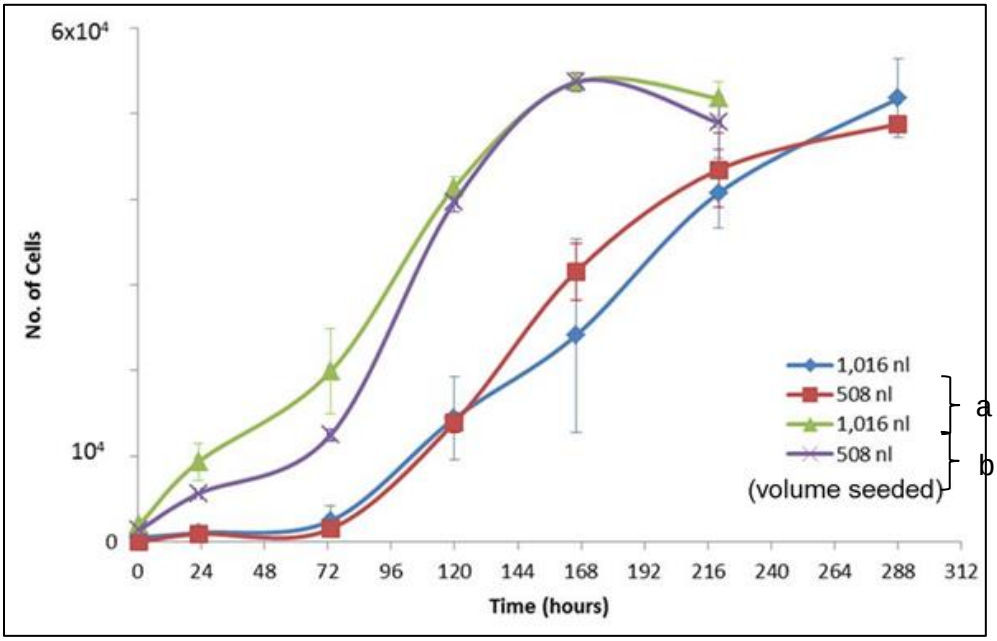

Figure 25. Plot of inkjet printed epithelial cells using HP printer 690 (a) and HP printer 340(b). n=2

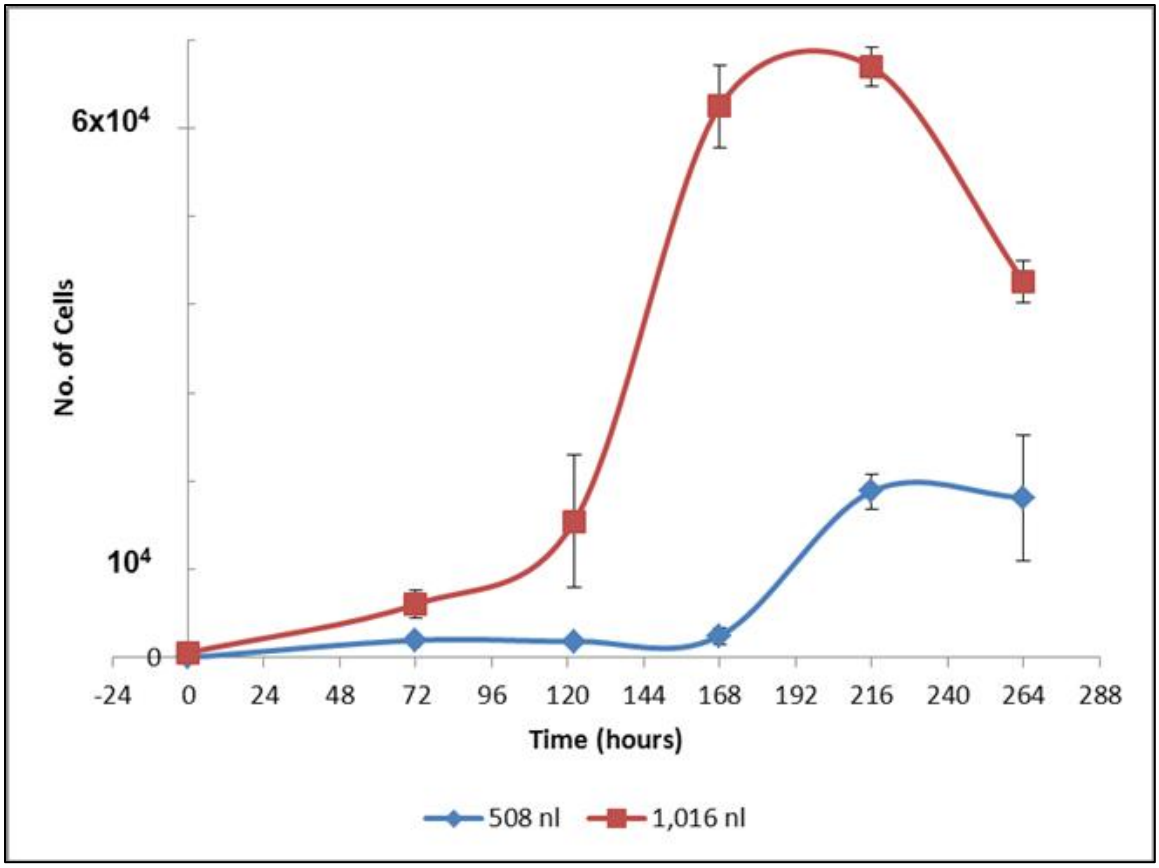

Figure 26. Plot of inkjet printed HepG2 cells using HP printer 340. N=2

6.4 Conclusions

The HepG2 and epithelial cells were successfully printed through the nozzles of a modified inkjet printer. The printed cells were deposited onto 96-well plates top off with culture medium to evaluate proliferation growth for high throughput screening. The proliferation analysis of epithelial and HepG2 cells showed that full confluency was attained indicating that cells remain viable upon exposure to the firing mechanism used in the inkjet printing systems. With the known benefits of high throughput and flexibility, this technology offers researchers a cost-effective tool to rapidly develop drug screening platforms.

CHAPTER 7: CONCLUSIONS

An inkjet based screening platform was evaluated for capability in miniturizing drug screening assays. We identifyied the apropiate dosage and treatment *in* vitro for two cell types and two common chemotherapeutic drugs DCA and cytoxan. We have demonstrated that this inkjet printing method can effectively deliver reliable cell and drug volumes at level of hundreds of picoliters, 180 $\pm$ 26%.

It was proven that using the inkjet printing technology similar outcomes than the standard micropipetting technique, in particular inhibitory concentrations IC50. However, the similarity was not as close related for the inhibitory concentration at 90% or IC90. While it was expected that DCA would not have as much effect on epithelial cells as in cancerous cells we found that DCA produce apoptosis at lower concentration dosage than commonly used chemotherapeutic drugs, cytoxan. We observed that both cell lines were inhibited, indicating that drugs used during the screening process did not have the selective effect towards cancerous cell bodies that was expected. Inkjet printing technology resulted in an accurate and reproducible dispensing of the drugs onto arrayed areas. Moreover, we observed reduced screening processing time since the inkjetting process eliminated many of the additional steps that are necessary in conventional screening.

7.1 Impact of the Work

Inkjet printing shows potential to reduce cost associated with the expenditure of costly reagents and compounds compared to traditional robotic systems as shown

shown in Table 4, In addition, the 24 h processing time can be reduced down to minutes due to the high speed that inkjet technologies offer.

Table 4. Outcomes comparison for traditional pipette-based robotic systems and the proposed inkjet printing platform.

Characteristic	Robotic	Printed
Mechanism	**Extrusion, contact**	**Ink-jetting, no contact**
Volume	**2 μl**	**180 pl**
Price ($)	200 (assumed)	0.018
Throughput	**0.2M assays/day**	**18M assays/day**
Screening time	24 hours (assumed)	16 in

7.3 Future Work

Next natural work for this research is to make it a clinical reality by creating a clinical trial with biopsied tissue samples from patients that can further benefit from the screening platform herein described. It is well-known that chemotherapies affect rapidly growing cells such as bone marrow, increasing the significance of predicting the possible growth inhibition on normal and stem cell lines in order to help minimize side effects.

In vitro studies have limited translation to clinical outcomes; therefore the design of a platform that closely mimics the body environment is required. A possible approach can be via creation of 3D organoids structures made of cocktail of different cells and factors encounter in human body. Exposure of drug regimens under these conditions will further develop the area of anticancer drug screening.

It is recommended to run a more holistic experiment where multiple drugs can be screen over cancerous and regular primary cell lines. Along with a deeper analyst that include synergistic, antagonistic, or additive effects. Understanding the role of the drug exposure period is a key on screening process as the one herein described.

Direct inkjet printing has shown potential on minimizing volumes used during screening processes to level down to picoliter; however, further development of the technology is required to be adapted in a closer relation to the proposed application. Development of inkjet system for regular ink printing involved challenges such as ink formulation, substrate control, computer modulation, and development of cleaning

stations to assure continuous function of the system. It is suggested that further development is required in each of these areas identified to further succeed in implementing inkjet technology into biotechnological applications.

REFERENCES

1. Rodriguez-Devora, J.I., et al., *High throughput miniature drug-screening platform using bioprinting technology.* Biofabrication, 2012. 4(3): p. 035001.
2. Technology, P.s.C.o.A.o.S.a. (2008) *Priorities for Personalized Medicine*.
3. Healthcare, F.K. *What is Personalized Medicine?* [cited 2012 March 2012]; Available from: http://www.ageofpersonalizedmedicine.org/what_is_personalized_medicine/.
4. Piccart-Gebhart, M.J., et al., *Trastuzumab after adjuvant chemotherapy in HER2-positive breast cancer.* N Engl J Med, 2005. 353(16): p. 1659-72.
5. Weston, A.D. and L. Hood, *Systems biology, proteomics, and the future of health care: toward predictive, preventative, and personalized medicine.* J Proteome Res, 2004. 3(2): p. 179-96.
6. John, R.M. and H. Ross, *Global Economic Cost of Cancer*, in *ICC World Cancer Congress*. 2010: Shenzhen, China.
7. Rodriguez-Devora, J.I., Z.D. Shi, and T. Xu, *Direct assembling methodologies for high-throughput bioscreening.* Biotechnol J, 2011.
8. Pignataro, B., *Nanostructured molecular surfaces: advances in investigation and patterning tools.* Journal of Materials Chemistry, 2009. 19(21): p. 3338-3350.
9. DiMasi, J.A., R.W. Hansen, and H.G. Grabowski, *The price of innovation: new estimates of drug development costs.* Journal of Health Economics, 2003. 22(2): p. 151-185.
10. Tollman, P., et al. (2001) *A Revolution in R&D How Genomics and Genetics are Transforming the Biopharmaceutical Industry*.
11. Lemmo, A.V., D.J. Rose, and T.C. Tisone, *Inkjet dispensing technology: applications in drug discovery.* Current Opinion in Biotechnology, 1998. 9(6): p. 615-617.
12. Brandish, P.E., et al., *A cell-based ultra-high-throughput screening assay for identifying inhibitors of D-amino acid oxidase.* Journal of Biomolecular Screening, 2006. 11(5): p. 481-7.
13. Mosser, S. (2006) *Achieving Low-Volume Liquid Handling*. GEN Genetic Engineering & Biotechnology News 26.
14. Mayr, L.M. and D. Bojanic, *Novel trends in high-throughput screening.* Curr Opin Pharmacol, 2009. 9(5): p. 580-8.
15. van't Veer, L.J. and R. Bernards, *Enabling personalized cancer medicine through analysis of gene-expression patterns.* Nature, 2008. 452(7187): p. 564-70.
16. American Cancer Society., *Cancer facts & figures*. 2012, The Society: Atlanta, GA. p. v.
17. Institute, N.C. (2012) *Common Cancer Types*.
18. Yoshitomi, S., et al., *Establishment of the transformants expressing human cytochrome P450 subtypes in HepG2, and their applications on drug metabolism and toxicology.* Toxicol In Vitro, 2001. 15(3): p. 245-56.

19. Freshney, R.I. and M.G. Freshney, *Culture of epithelial cells*. 2nd ed. Culture of specialized cells. 2002, New York: Wiley-Liss. xv, 461 p.
20. Atkins, J.H. and L.J. Gershell, *Selective anticancer drugs.* Nat Rev Drug Discov, 2002. 1(7): p. 491-2.
21. Bartal, A., et al., *[Novel oral anticancer drugs: a review of adverse drug reactions, interactions and patient adherence].* Orv Hetil, 2012. 153(2): p. 66-78.
22. Zhu, F., et al., *Trends in the exploration of anticancer targets and strategies in enhancing the efficacy of drug targeting.* Curr Mol Pharmacol, 2008. 1(3): p. 213-32.
23. Spencer, P. and W. Holt, *Anticancer drugs : design, delivery and pharmacology*. Cancer etiology, diagnosis and treatments. 2009, New York: Nova Biomedical Books. xi, 271 p.
24. Powis, G., *Anticancer drugs : reactive metabolism and drug interactions*. 1st ed. International encyclopedia of pharmacology and therapeutics. 1994, Oxford, England ; New York: Pergamon Press. xv, 444 p.
25. Innocenti, F., *Genomics and pharmacogenomics in anticancer drug development and clinical response*. Cancer drug discovery and development. 2008, Totowa, NJ: Humana. xiv, 377 p.
26. Salmon, S.E. and A.C. Sartorelli, *Cancer Chemotherapy, in Basic and Clinical Pharmacology*. Appleton-Lange, ed. B.G. Katzung. 1998. p. 881-911.
27. Calabresi, P. and B.A. Chabner, *Chemotherapy of Neoplastic Diseases. In, Goodman and Gillman's The Pharmacologial Basis of Therapeutics*, ed. J.G. Hardman, et al. 1996: TheMcGraw-Hill Companies, Inc.
28. Chabner, B.A., et al., *Antineoplastic Agents. In, Goodman and Gillman's The Pharmacologial Basis of Therapeutics*, ed. J.G. Hardman, et al. 1996: TheMcGraw-Hill Companies, Inc. pp.1233-1286.
29. The American Society of Health-System Pharmacists, I., *Cyclophosphamide*, U.N.L.o. Medicine, Editor. 2011, PubMed Health.
30. Michael Gordon, P.D. (2011) *Cancer Chemotherapy: Drug Classification and Mechanism of Action*. Medical Pharmacology and Disease-Based
31. Omudhome Ogbru, P. (2012) *Cyclophosphamide - oral, Cytoxan*.
32. Warburg, O., *On the origin of cancer cells.* Science, 1956. 123(3191): p. 309-14.
33. Gudi, R., et al., *Diversity of the pyruvate dehydrogenase kinase gene family in humans.* J Biol Chem, 1995. 270(48): p. 28989-94.
34. Bonnet, S., et al., *A mitochondria-K+ channel axis is suppressed in cancer and its normalization promotes apoptosis and inhibits cancer growth.* Cancer Cell, 2007. 11(1): p. 37-51.
35. Wong, J.Y., et al., *Dichloroacetate induces apoptosis in endometrial cancer cells.* Gynecol Oncol, 2008. 109(3): p. 394-402.
36. Stacpoole, P.W., et al., *Controlled clinical trial of dichloroacetate for treatment of congenital lactic acidosis in children.* Pediatrics, 2006. 117(5): p. 1519-31.
37. Kaufmann, P., et al., *Dichloroacetate causes toxic neuropathy in MELAS: a randomized, controlled clinical trial.* Neurology, 2006. 66(3): p. 324-30.

38. Pearson, H., *Cancer patients opt for unapproved drug.* Nature, 2007. 446(7135): p. 474-5.
39. Sun, R.C., et al., *Reversal of the glycolytic phenotype by dichloroacetate inhibits metastatic breast cancer cell growth in vitro and in vivo.* Breast Cancer Res Treat, 2010. 120(1): p. 253-60.
40. Jensen, G.C., et al., *Inkjet-printed gold nanoparticle electrochemical arrays on plastic. Application to immunodetection of a cancer biomarker protein.* Phys Chem Chem Phys, 2011. 13(11): p. 4888-94.
41. Abe, K., et al., *Inkjet-printed paperfluidic immuno-chemical sensing device.* Anal Bioanal Chem, 2010. 398(2): p. 885-93.
42. Rodriguez-Devora, J.I. and T. Xu, *Fabrication of Miniature Drug Screening Platform Using Low Cost Bioprinting Technology.* NIP 26 2010: p. 574-577.
43. Arrabito, G. and B. Pignataro, *Inkjet printing methodologies for drug screening.* Anal Chem, 2010. 82(8): p. 3104-7.
44. Xu, T., et al., *Inkjet printing of viable mammalian cells.* Biomaterials, 2005. 26(1): p. 93-9.
45. Xu, T., et al., *Viability and electrophysiology of neural cell structures generated by the inkjet printing method.* Biomaterials, 2006. 27(19): p. 3580-8.
46. Saunders, R.E., J.E. Gough, and B. Derby, *Delivery of human fibroblast cells by piezoelectric drop-on-demand inkjet printing.* Biomaterials, 2008. 29(2): p. 193-203.
47. Roth, E.A., et al., *Inkjet printing for high-throughput cell patterning.* Biomaterials, 2004. 25(17): p. 3707-15.
48. Miller, E.D., et al., *Dose-dependent cell growth in response to concentration modulated patterns of FGF-2 printed on fibrin.* Biomaterials, 2006. 27(10): p. 2213-21.
49. Ilkhanizadeh, S., A.I. Teixeira, and O. Hermanson, *Inkjet printing of macromolecules on hydrogels to steer neural stem cell differentiation.* Biomaterials, 2007. 28(27): p. 3936-43.
50. Yamazoe, H. and T. Tanabe, *Cell micropatterning on an albumin-based substrate using an inkjet printing technique.* Journal of Biomedical Materials Research Part A, 2009. 91(4): p. 1202-9.
51. Xu, T., et al., *Viability and electrophysiology of neural cell structures generated by the inkjet printing method.* Biomaterials, 2006. 27(19): p. 3580-3588.
52. Xu, T., et al., *Inkjet printing of viable mammalian cells.* Biomaterials, 2005. 26(1): p. 93-99.
53. Zarowna-Dabrowska, A., et al., *Generation of primary hepatocyte microarrays by piezoelectric printing.* Colloids Surf B Biointerfaces, 2012. 89: p. 126-32.
54. DiMasi, J.A., R.W. Hansen, and H.G. Grabowski, *The price of innovation: new estimates of drug development costs.* J Health Econ, 2003. 22(2): p. 151-85.
55. Boland, T., et al., *Drop-on-demand printing of cells and materials for designer tissue constructs.* Materials Science & Engineering C-Biomimetic and Supramolecular Systems, 2007. 27(3): p. 372-376.

56. Xu, T., et al., *Construction of high-density bacterial colony arrays and patterns by the ink-jet method.* Biotechnol Bioeng, 2004. 85(1): p. 29-33.
57. Nakamura, M., et al., *Biocompatible inkjet printing technique for designed seeding of individual living cells.* Tissue Engineering, 2005. 11(11-12): p. 1658-66.
58. Yan, Y., et al., *Fabrication of viable tissue-engineered constructs with 3D cell-assembly technique.* Biomaterials, 2005. 26(29): p. 5864-71.
59. Barron, J.A., et al., *Biological laser printing: a novel technique for creating heterogeneous 3-dimensional cell patterns.* Biomed Microdevices, 2004. 6(2): p. 139-47.
60. Duocastella, M., et al., *Study of the laser-induced forward transfer of liquids for laser bioprinting.* Appl Surf Sci, 2007. 253(19): p. 7855-7859.
61. Hopp, B., et al., *Survival and proliferative ability of various living cell types after laser-induced forward transfer.* Tissue Eng, 2005. 11(11-12): p. 1817-1823.
62. Anderson, D.G., S. Levenberg, and R. Langer, *Nanoliter-scale synthesis of arrayed biomaterials and application to human embryonic stem cells.* Nat Biotechnol, 2004. 22(7): p. 863-6.
63. Ito, A., et al., *Magnetic force-based cell patterning using Arg-Gly-Asp (RGD) peptide-conjugated magnetite cationic liposomes.* J Biosci Bioeng, 2007. 104(4): p. 288-93.
64. MacBeath, G. and S.L. Schreiber, *Printing proteins as microarrays for high-throughput function determination.* Science, 2000. 289(5485): p. 1760-3.
65. Tavana, H., et al., *Nanolitre liquid patterning in aqueous environments for spatially defined reagent delivery to mammalian cells.* Nat Mater, 2009. 8(9): p. 736-41.
66. Derby, B., R. Saunders, and J. Gough, *Damage to biological materials during ink-jet printing.* Nip 23: 23rd International Conference on Digital Printing Technologies, Technical Program and Proceedings/Digital Fabrication 2007, 2007: p. 944-944.
67. Moon, S., et al., *Layer by layer three-dimensional tissue epitaxy by cell-laden hydrogel droplets.* Tissue Eng Part C Methods, 2010. 16(1): p. 157-66.
68. Hong, J., J.B. Edel, and A.J. deMello, *Micro- and nanofluidic systems for high-throughput biological screening.* Drug Discov Today, 2009. 14(3-4): p. 134-146.
69. Bu, M.Q., et al., *Characterization of a microfluidic magnetic bead separator for high-throughput applications.* Sensors and Actuators a-Physical, 2008. 145: p. 430-436.
70. Albrecht, D.R., et al., *Probing the role of multicellular organization in three-dimensional microenvironments.* Nat Methods, 2006. 3(5): p. 369-75.
71. Lee, K.B., et al., *The use of nanoarrays for highly sensitive and selective detection of human immunodeficiency virus type 1 in plasma.* Nano Lett, 2004. 4(10): p. 1869-1872.
72. Jing, G., et al., *Cell patterning using molecular vapor deposition of self-assembled monolayers and lift-off technique.* Acta Biomater, 2011. 7(3): p. 1094-103.

73. Benson, H.J., *Benson's microbiological applications : laboratory manual in general microbiology*. 10th ed. 2007, Boston: McGraw-Hill Higher Education. xiv, 544 p.
74. Atala, A., et al., *Injectable alginate seeded with chondrocytes as a potential treatment for vesicoureteral reflux.* J Urol, 1993. 150(2 Pt 2): p. 745-7.
75. Lehr, H.A., et al., *Complete chromogen separation and analysis in double immunohistochemical stains using Photoshop-based image analysis.* J Histochem Cytochem, 1999. 47(1): p. 119-26.
76. Gronemeyer, S.A., et al., *Fast adipose tissue (FAT) assessment by MRI.* Magn Reson Imaging, 2000. 18(7): p. 815-8.
77. Loughlin, P.M., et al., *Quantifying tumour-infiltrating lymphocyte subsets: a practical immuno-histochemical method.* Journal of Immunological Methods, 2007. 321(1-2): p. 32-40.
78. Chorghade, M.S., *Drug discovery and development*. 2006, Hoboken, N.J.: Wiley-Interscience.
79. Freshney, R.I., *Culture of animal cells : a manual of basic technique and specialized applications*. 6th ed. 2010, Hoboken, N.J.: Wiley-Blackwell. xxxi, 732 p., 28 p. of plates.
80. Ma, J. and D.J. Waxman, *Collaboration between hepatic and intratumoral prodrug activation in a P450 prodrug-activation gene therapy model for cancer treatment.* Molecular Cancer Therapeutics, 2007. 6(11): p. 2879-2890.
81. Mohebi, M.M. and J.R. Evans, *A drop-on-demand ink-jet printer for combinatorial libraries and functionally graded ceramics.* J Comb Chem, 2002. 4(4): p. 267-74.
82. Lemmo, A.V., D.J. Rose, and T.C. Tisone, *Inkjet dispensing technology: applications in drug discovery.* Curr Opin Biotechnol, 1998. 9(6): p. 615-7.
83. Collier, W.A., D. Janssen, and A.L. Hart, *Measurement of soluble L-lactate in dairy products using screen-printed sensors in batch mode.* Biosens Bioelectron, 1996. 11(10): p. 1041-9.
84. Hughes, T.R., et al., *Expression profiling using microarrays fabricated by an ink-jet oligonucleotide synthesizer.* Nat Biotechnol, 2001. 19(4): p. 342-7.
85. Strober, W., *Trypan blue exclusion test of cell viability.* Curr Protoc Immunol, 2001. Appendix 3: p. Appendix 3B.
86. Jemal, A., et al., *Cancer statistics, 2002.* CA Cancer J Clin, 2002. 52(1): p. 23-47.
87. Michelakis, E.D., L. Webster, and J.R. Mackey, *Dichloroacetate (DCA) as a potential metabolic-targeting therapy for cancer.* Br J Cancer, 2008. 99(7): p. 989-94.

Appendix A: Cancer Facts

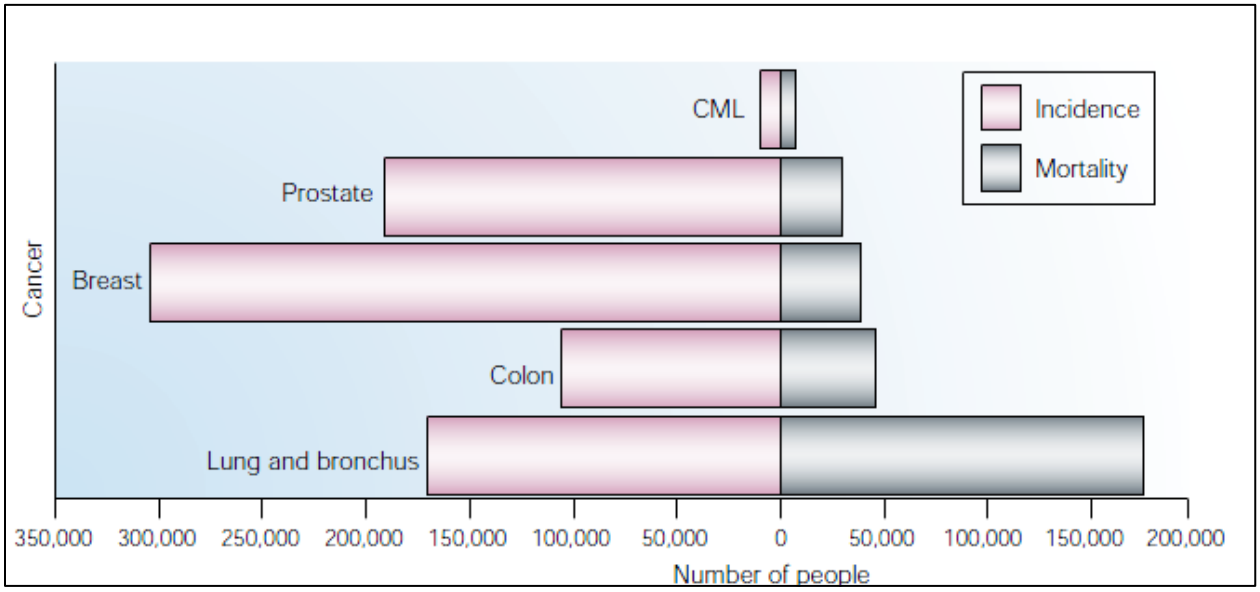

Figure 27. Incidence and mortality of selected cancers in the United Stated in 2002 [20]. Data taken from [86].

Appendix B: DCA Controversy

In January 2007, researchers from the University Alberta published a study showing that DCA was able to slow the growth of cancer cells from the lung, breast, and brain *in vitro* [87]. This study found that laboratory rats that had DCA in their drinking water had much slower tumor growth than those not treated with DCA. Some news and Internet outlets reported on the study. To some, the story held out hope for a cancer cure. The story received widespread attention, implying that an affordable, safe treatment was available but because DCA couldn't be patented, no one would study it.

Because it is not FDA approved drug, only doctors doing research on DCA can prescribe it. But the interest in DCA after the 2007 study led to some companies selling DCA directly to patients over the Internet. The FDA became involved, since sellers were marketing a drug that hadn't been proven, and that was not approved for sales or marketing in the U.S. On those grounds, the FDA has stopped at least one shipment of DCA from entering the United States (cancer.org).

Appendix C: MTS Based Drug Cytotoxicity Protocol

Incubate monolayer cultures in microtitration plates in a range of drug concentrations (Fig. 21.5). Remove the drug, and feed the plates daily for two to three PDTs; then feed the plates again, and add MTS to each well. Incubate the plates in the dark for 4 h, and then remove the medium and MTS. Dissolve the water-insoluble MTS-formazan crystals in DMSO, add a buffer to adjust the final pH, and record the absorbance in a plate reader.

Materials required:

Sterile:

- Growth medium
- Trypsin (0.25% + EDTA, 1 mM, in PBSA)
- MTS: tetrazolium compound [3-(4,5-dimethylthiazol-2-yl)-5-(3-carboxymethoxyphenyl)-2-(4-sulfophenyl)-2H-tetrazolium, inner salt
- Sorensen's glycine buffer (0.1 M glycine, 0.1 M NaCl adjusted to pH 10.5 with 1 M NaOH)
- Microtitration plates
- Pipette tips, preferably in an autoclavable tip box
- Petri dishes (non–TC-treated), 5 cm and 9 cm or reservoir (Corning)
- Universal containers or tubes, 30 mL and 100 mL

Non-sterile:

- Plastic box (clear polystyrene, to hold plates)
- Multichannel pipettor
- Dimethyl sulfoxide (DMSO)
- Microplate Dispenser
- ELISA plate reader
- Plate carrier for centrifuge (for cells growing in suspension; see Appendix II: Microtitration Plate Centrifugation)

Procedure:

Plating out cells

1. A subconfluent monolayer culture was trypsinized, and cells were collected in growth medium containing serum.

2. The suspension was centrifuged (5 min at 200 g) to pellet the cells. Cells were resuspend in growth medium, and count them.

3. Cells were diluted to 2.5 to 50 × 103 cells/mL, depending on the growth rate of the cell line, and allowing 20 mL of cell suspension per microtitration plate.

4. Transfer the cell suspension to a 9-cm Petri dish, and, with a multichannel pipette, add 200 µL of the suspension into each well of the central 10 columns of a flat-bottomed 96-well plate (80 wells per plate), starting with column 2 and ending with column 11, placing 0.5 to 10 × 103 cells into each well.

5. Add 200 μL of growth medium to the eight wells in columns 1 and 12. Column 1 will be used to blank the plate reader; column 12 helps maintain the humidity for column 11 and minimizes the ‘‘edge effect.’’

6. Put the plates in a plastic lunch box, and incubate in a humidified atmosphere at 37◦C for 1 to 3 days, such that the cells are in the exponential phase of growth at the time that drug is added.

7. For non-adherent cells, prepare a suspension in fresh growth medium. Dilute the cells to 5 to 100 × 103 cells/mL, and plate out only 100 μL of the suspension into round-bottomed 96-well plates. Add drug immediately to these plates.

Drug addition

8. Prepare a serial fivefold dilution of the cytotoxic drug in growth medium to give eight concentrations. This set of concentrations should be chosen such that the highest concentration kills most of the cells and the lowest kills none of the cells. Once the toxicity of a drug is known, a smaller range of concentrations can be used. Normally three plates are used for each drug to give triplicate determinations within one experiment.
9. For adherent cells:

   (a) Remove the medium from the wells in columns 2 to 11. This can be achieved with a hypodermic needle attached to a suction line.

(b) Feed the cells in the eight wells in columns 2 and 11 with 200 µL of fresh growth medium; these cells are the controls.

(c) Transfer the drug solutions to 5-cm Petri dishes, and add 200 µL to each group of four wells with a four-tip pipettor.

(d) Add the cytotoxic drug to the cells in columns 3 to 10. Only four wells are needed for each drug concentration, such that rows A through D can be used for one drug and rows E through H for a second drug.

10. Return the plates to the plastic box, and incubate them for a defined exposure period.

Growth period

11. At the end of the drug exposure period, remove the medium from all of the wells containing cells, and feed the cells with 200 µL of fresh medium. Centrifuge plates containing non-adherent cells (5 min at 200 g) to pellet the cells. Then remove the medium, using a fine-gauge needle to prevent disturbance of the cell pellet.
12. Feed the plates daily for 2 to 3 PDTs. Estimation of surviving cell numbers
13. Feed the plate with 200 µL of fresh medium at the end of the growth period, and add 50 µL of MTS to all of the wells in columns 1 to 11.
14. Wrap the plates in aluminum foil, and incubate them for 4 h in a humidified atmosphere at 37º C. Note that 4 h is a minimum incubation time, and plates can be left for up to 8 h.

15. Remove the medium and MTS from the wells (centrifuge for non-adherent cells), and dissolve the remaining MTS-formazan crystals by adding 200 µL of DMSO to all of the wells in columns 1 to 11.
16. Add glycine buffer (25 µL per well) to all of the wells containing DMSO.
17. Record absorbance at 490 nm immediately, because the product is unstable. Use the wells in column 1, which contain medium and MTS but no cells, to blank the plate reader.

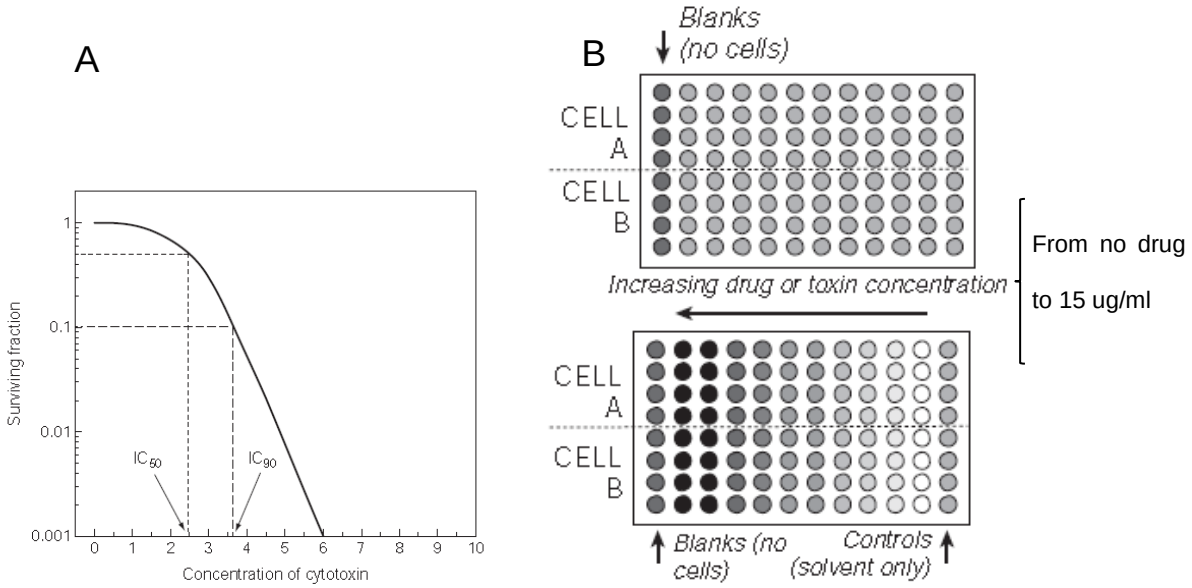

Figure 28. A) Semi-log plot of standard dose-response curve. B) Microtitration assay on 96-well plate.

Appendix D: Drug Solvent Analysis and Inhibitory Concentration for Drug Screening Process

The inhibitory effect of cells exposed to cyclophosphamide monohydrate and dichloroacetate (DCA) at a concentration of 10.563 and 5.157 mM is shown in Figure 29. It was found that when the drugs were dissolved in PBS no inhibitory effect was observed, suggesting drugs insolubility in PBS. As expected, DMSO-dissolved drugs inhibited cell growth at approximately 50 percent when concentrations were 10.563 mM in cytoxan and 5.157 mM in DCA.

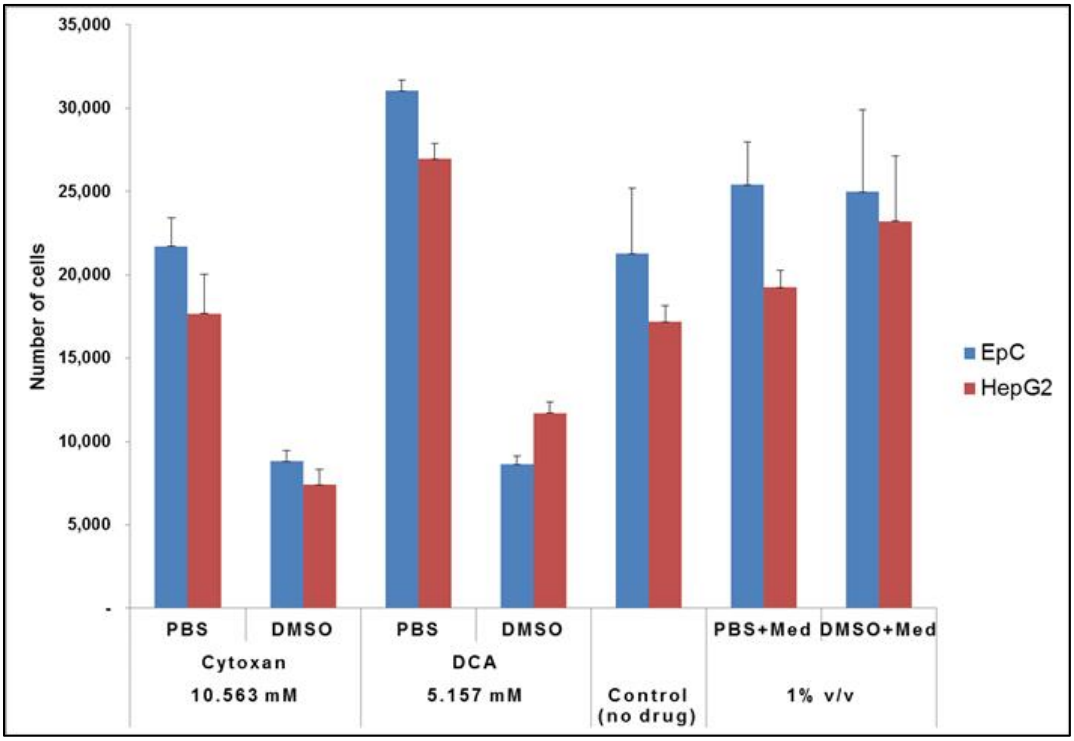

Figure 29. Number of cells per well when exposed to cyclophosphamide monohydrate and dichloroacetate (DCA) at a concentration of 10.563 and 5.157 mM, respectively. DMSO and PBS were used as drug solvents, controls in the far right report data on cytotoxicity when exposed to only medium (EMEM), 1% PBS in EMEM, and 1% DMSO in EMEM. n=3

The lack of any gradient on the dose-response curve when drugs were dissolved in PBS indicates a solubility problem of the PBS with used chemotherapeutic drugs. Therefore, PBS was not a suitable solvent for the drugs herein investigated.

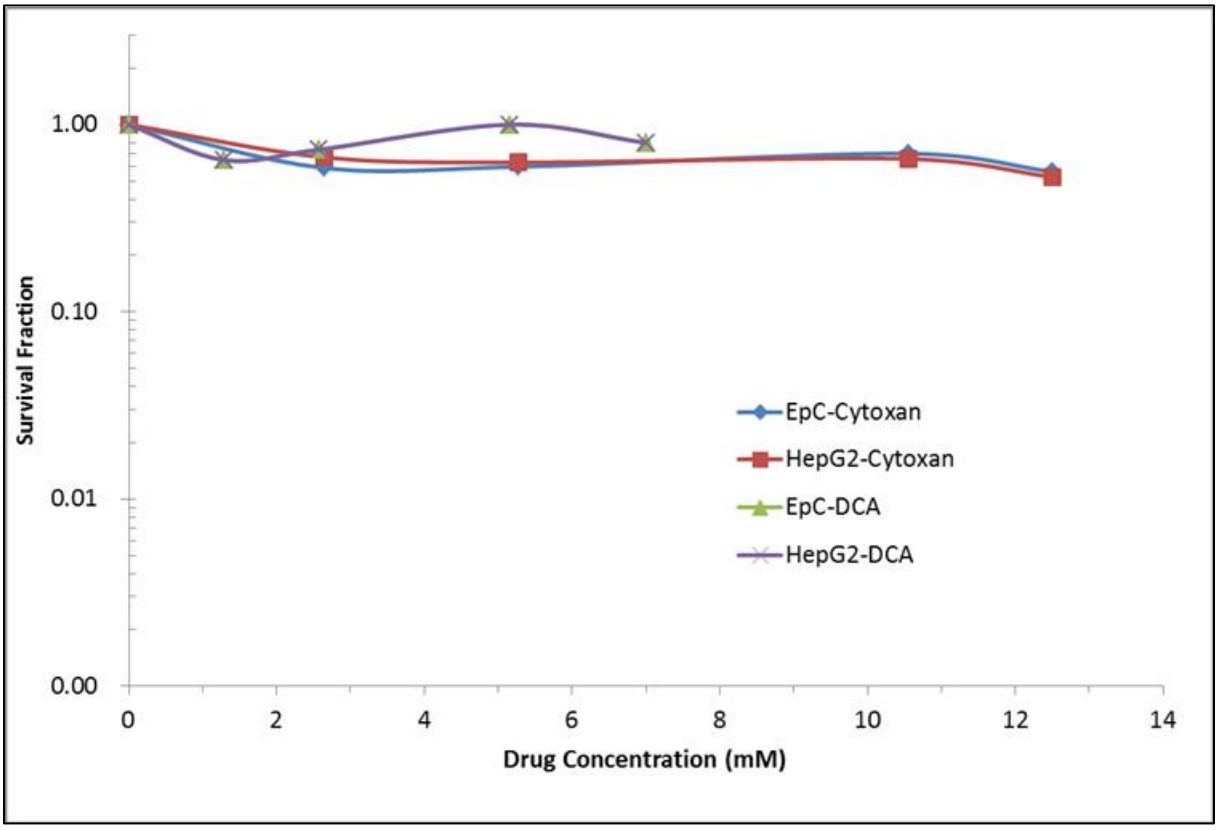

Figure 30. Dose-response curves by micropipetting technique. Survival fraction of epithelial and HepG2 cell lines under Cytoxan and dichloroacetate treatment at increasing concentrations when diluted in phosphate buffer saline (PBS). n=3

Appendix E: Drug Screening using Inkjet printing – Single Round

Figure 31 show the survival fraction of cells after drug exposure. A hill around 4mM was observed for cell lines exposed to DCA, while for cell lines exposed to cytoxan the hill was around 6mM. These observations were expected and were reported before in the literature[39]. At higher concentrations, the data suggest that inhibition was increasing with dosage; however, at further increased concentrations, the cells fully recovered. This suggests that the inkjet nozzles may have been clogged. Printing direction is illustrated by arrow located at bottom of Figure 31.

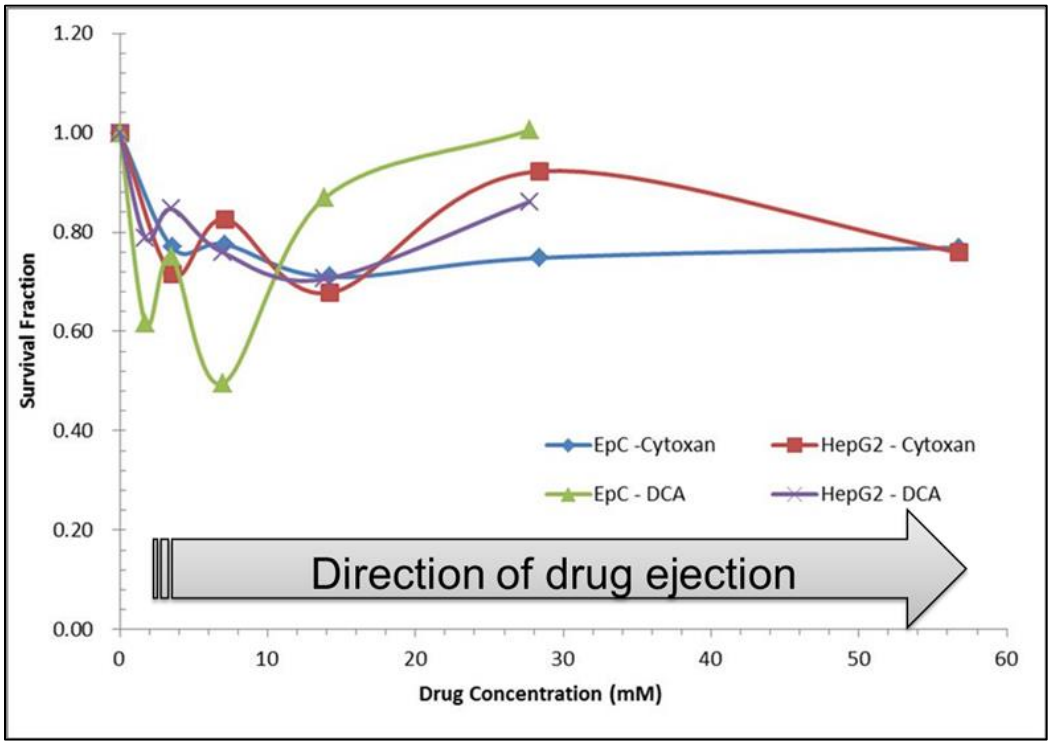

Figure 31. Dose-response curves by inkjet printing technique. Survival fraction of epithelial and HepG2 cell lines under cytoxan and dichloroacetate treatment at increasing concentrations when diluted in dimethyl sulfate oxide (DMSO). n=3. Identification of half maximal and 90% inhibitory concentrations (IC50 and IC90).

CURRICULUM VITA

Jorge earned his bachelor in engineering in Electrical and Mechanical Engineering from his Hometown University the Technological Institute of Ciudad Juarez in 2005. He served over six years as Product Engineer in Automotive industry. He received his Master of Science degree in Mechanical Engineering in 2010 from the University of Texas at El Paso. His research interests lie in the area of regenerative medicine, tissue engineering, drug delivery systems, and drug screening platforms.

Dr. Rodriguez's academic outcomes include: four peer-reviewed publications, one patent, three book chapters, seven presentations on international conferences and six on local conferences, plus mentorship of over 10 students. He will continue growing his publications through a postdoctoral position.

Dr. Rodriguez's dissertation entitled "Inkjet Based Personalized Screening Platform for Cancer Therapy" was supervised by Dr. Thomas Boland and Dr. Tao Xu.

Permanent Address:

Región de Porto 1024-12, Jardines de San Carlos I

Ciudad Juárez, Chihuahua, México 32563